NBER WORKING PAPER SERIES

THE IMPACT OF CLIMATE CHANGE ON FISHERIES

Fabio Cevenini
Christopher Costello
Carlo Fezzi

Working Paper 35994
http://www.nber.org/papers/w35994

NATIONAL BUREAU OF ECONOMIC RESEARCH
1050 Massachusetts Avenue
Cambridge, MA 02138
November 2026

We are grateful to Clementina Crocè, Thijs Dekker, Olivier Deschenes, Don Fullerton, Elie Murard, Hélène Ollivier, Claudia Kelsall, Catharina Latka, Roman Sieler, Joseph Shapiro, Marco Tomasi and Guglielmo Zappalà for valuable feedback. We thank participants at the Econometric Society ESIF-CLIM Conference, EmLab seminars at the University of California, Santa Barbara, and the Early Career Workshop on Applied Environmental and Climate Change Economics at Fondazione Enrico Mattei (Milan) for insightful discussions. We also thank the Bartlett School at University College London, the LEEP Institute at the University of Exeter, the Department of Economics at the University of Florence, the Center for Development Research (ZEF) at the University of Bonn, the Max Planck Institute for Biology in Tübingen, and the Centre for Social and Economic Research on the Global Environment (CSERGE) at the University of East Anglia for the valuable comments and feedback received during seminars hosted by these institutions. We thank Chiara Piroddi for sharing the Mixed trophic Impact matrices for the Mediterranean area, and Simone Libralato for assistance with the Ecopath with Ecosim software. Fabio Cevenini also acknowledges financial and institutional support from the SUSTEEMS PhD programme at the University of Trento. All the remaining errors are our own. The views expressed herein are those of the authors and do not necessarily reflect the views of the National Bureau of Economic Research.

NBER working papers are circulated for discussion and comment purposes. They have not been peer-reviewed or been subject to the review by the NBER Board of Directors that accompanies official NBER publications.

© 2026 by Fabio Cevenini, Christopher Costello, and Carlo Fezzi. All rights reserved. Short sections of text, not to exceed two paragraphs, may be quoted without explicit permission provided that full credit, including © notice, is given to the source.

The Impact of Climate Change on Fisheries
Fabio Cevenini, Christopher Costello, and Carlo Fezzi
NBER Working Paper No. 35994
November 2026
JEL No. Q22, Q54

ABSTRACT

This paper provides the first causal estimate of the effect of ocean temperature variations on fishing revenue. We develop a simple theoretical model underpinning an empirical specification estimated on 2.5 million spatially explicit observations of fishing revenue from all European vessels for 2013–2022. The identification strategy leverages a novel metric, Marine Degree Days, which quantifies species-specific temperature exposure relative to biologically established thermal tolerance intervals. Within this framework we address key identification challenges, including spatial selection and ecological interdependencies across species. We find that deviations from species' thermal preferences lead to significant losses in fishing revenue, with heat exposure causing the most pronounced impacts. These effects are mediated by species' vertical mobility and ecological characteristics. Projections across different climate scenarios point to widespread revenue declines by 2100, reaching €560 million annual losses in the warmest scenario, though impacts are highly spatially heterogeneous. Lower-income, equatorial areas are expected to suffer the most, while some colder regions experience gains.

Fabio Cevenini
University of Trento
Department of Economics
fabio.cevenini@unitn.it

Carlo Fezzi
University of Trento
Department of Economics
carlo.fezzi@unitn.it

Christopher Costello
University of California, Santa Barbara
Bren School of Environmental Science
& Management,
and Department of Economics
and NBER
costello@bren.ucsb.edu

An online appendix is available at http://www.nber.org/data-appendix/w35994

1 Introduction

There is mounting evidence on the effects of weather and climate on economic outcomes, such as agricultural output (Burke & Emerick, 2016; Moscona & Sastry, 2023; Schlenker et al., 2006; Waldinger, 2022), labour productivity (Graff Zivin & Neidell, 2014; Somanathan et al., 2021) and economic growth (Acevedo et al., 2020; Bilal & Känzig, 2026; Dell et al., 2012). Temperature changes have been found to have a tangible impact also on mortality (Carleton et al., 2022; Deschênes & Greenstone, 2011), violence (Card & Dahl, 2011; Harari & Ferrara, 2018) and mental health (Burke et al., 2018). These studies have shaped both scientific and policy debates by translating current and future climatic variation into economic impacts (see Auffhammer, 2018; Carleton and Hsiang, 2016; Dell et al., 2014 for reviews). Yet, this empirical literature has largely overlooked the ocean, despite its central role in both the climatic and economic systems. As a result, we still know relatively little about the economic consequences of global warming on marine fisheries, one of the world's most important natural production systems.

Marine fisheries generate hundreds of billions of dollars in revenue globally (FAO, 2025), supporting more than 62 million jobs worldwide across harvesting, processing, trade, and coastal services (FAO, 2024). They also sustain the livelihood of about 10% of the global population by playing a central role in food security, particularly in developing countries (Costello et al., 2020). Arguably, the scarcity of causal evidence on the impact of climate change on fisheries reflects two obstacles that characterize the marine environment. The first one is severe data limitations (Costello et al., 2012). Compared to terrestrial sectors like agriculture, fisheries outcomes have been recorded less consistently, are less standardized across countries, and often lack fine geographic detail, especially over long time spans. Second, the intrinsic complexities of the marine system pose unique challenges for causal identification. Fish stocks are not directly observed, can move across space, and interact dynamically with both their environment and other species. Finally, fishers' adaptation strategies respond not only to realized weather, but also to expected returns and to information about forthcoming conditions, such as weather forecasts, which can shape effort, timing, and location choices (Shrader, 2023; M. D. Smith, 2005). From an econometric perspective, these features introduce complex forms of sample selection, spillovers, and potential omitted variable bias that make standard empirical strategies difficult to implement.

This paper addresses this research gap by providing the first causal estimate of the effect of ocean temperature on marine fisheries revenue. We address the challenges above by leveraging a novel, high-resolution dataset including more than 2.5 million observations of annual, spatially-located fishing revenue, spanning the Atlantic Ocean, the Arctic, and the Mediterranean Sea. These spatial data contain information about the fishing activities carried out between 2013 and 2022 by the universe of vessels registered in countries belonging to the European Union, including records of all the species caught and the characteristics of the fishing fleet such as vessel length, fishing technique and fishing gear used. These metrics are stored at a 0.5 x 0.5 spatial grid resolution ($\sim$ 55 x 55 km at the equator) annually.

We merge these data with two other sources of information. First, recognizing that fish physiology depends on

temperature, we match each cell-year with its local thermal conditions represented by daily, remotely sensed, sea surface temperature (SST). Second, recognizing that warming may affect each species differently, we collect species-level biological information, most notably their thermal preference ranges (Cheung et al., 2013). These data enable us to map a single spatial temperature realization to the heterogeneous levels of exposure experienced by all the species residing in that location. Specifically, we translate SST into species-specific exposure by developing a novel metric inspired by the degree-day measure used in agricultural and energy economics (see Hogan and Schlenker, 2024 for an overview), which we call *Marine Degree Day* (MDD). This new indicator cumulates the exposure to temperatures outside the preferred thermal interval of each species. The key insight provided by this metric is that the same sea temperature can be beneficial for one species and harmful for another, depending on their different thermal tolerances. For each species, we consider the degree days above their thermal range (denoted by MDD^{+}) and the degree days below their thermal range (denoted by MDD^{-}). These measures reflect both the intensity and the duration of ocean temperature dynamics, while embedding biological and ecological heterogeneity in two easily interpretable indexes.

Our empirical design directly estimates the impact of MDDs on the fishing revenue for each species, exploiting the exogenous variation in exposure. Intuitively, the identification of the causal effect of temperature on fishing revenue comes from two underlying comparisons. First, our strategy compares outcomes for different species caught by the same vessel and technology types in the same location and year. Second, we compare revenue for the same species but in neighboring locations that contain the same management environment. In all analyses, we include a high-dimensional fixed-effects specification that absorbs (i) all determinants of revenue that vary at the cell-by-year level, such as fishers' selection and effort in different fishing locations, technology and local determinants such as the ecological habitat or the presence of a marine protected area, and (ii) all shocks that are common to the same species-by-year-by-management region, such as management constraints at the relevant regulatory scale and market conditions such as input and output prices.

Our empirical specification is underpinned by a stylized bio-economic model that links ocean temperature to fishing revenue through fish population dynamics. In this model, temperature shifts local habitat conditions and changes the system's carrying capacity, i.e. the amount of fish biomass the environment can sustain given its ecological limits. A change in carrying capacity alters biological growth and the evolution of biomass over time, which affects the sustainable harvest rate and, therefore, revenue. Our model maps temperature to biological growth via carrying capacity, while the sustainable management objectives from EU fishing regulations allow us to link changes in carrying capacity to changes in target biomass. This structural framework resolves our primary empirical problem: the inability to directly observe fish stocks.

We find that thermal exposure outside species' preferred ranges generates significant and asymmetric damages. Both heat and cold exposure generate reductions in fishing revenue, but the estimated effect of exposure above the range is approximately three times that of exposure below it. When we allow for non-linear effects, we find that the marginal effect of heat exposure becomes significantly more harmful at higher temperatures, confirming

that extremely warm conditions can generate disproportionate biological and economic impacts (Frölicher et al., 2018; K. E. Smith et al., 2023), while the damage from cold is approximately linear over the observed range of our data. We also document different sources of heterogeneity underpinned by plausible biological mechanisms of adaptation including vertical mobility in the water column and ecological group. These results remain coherent under a broad set of robustness checks, including potential spillovers across space, ecological spillovers across species, specifications that allow species-specific responses to habitat characteristics and spatial gradients, and many alternative specifications, variable definitions and samples.

Finally, we combine the estimated dose-response function with daily temperature projections under two different climate scenarios to quantify the implied consequences of ocean warming on fisheries revenue through 2100. Our projections imply widespread declines under higher-emissions pathways, with substantial spatial heterogeneity. Under the most pessimistic scenario, we project losses of approximately €560 million per year by the end of the century. Such losses are concentrated in already warm areas, while colder regions experience smaller damages or even gains. This spatial pattern implies that damages are disproportionately concentrated in areas with lower-income, highlighting a marine dimension of climate inequality that is largely absent from the existing literature (Cain et al., 2024).

Our findings extend the climate economics literature by providing the first direct causal estimate of the effect of ocean temperature on fisheries revenue. While a large scientific literature has documented the biological impacts of ocean warming on marine ecosystems (Cheung et al., 2013; Hoegh-Guldberg & Bruno, 2010; Sumaila et al., 2011), only a few studies have attempted to quantify its economic consequences (Barange et al., 2014; Cheung et al., 2010, 2021, 2026; Gaines et al., 2018; Lam et al., 2016). These contributions differ in their modeling details but share a common approach. They start from a biological model that translates ocean warming into predicted changes in biomass and potential catches, and then convert biological outcomes into economic ones by applying a back-of-the-envelope calculation assuming prices, fishing effort and management regimes as fixed. This *simulation-based* approach is useful for identifying vulnerable species and regions, but it does not rely on realized outcomes and therefore cannot capture fishers' adaptation or other complexities that are only revealed through careful empirical analysis. In particular, it abstracts from the ways in which changes in behavior, technology, and regulation mediate ecological pressures into realized catches and revenue. In contrast, our approach estimates how revenue responds to temperatures using realized data, so the effects we recover already embed the influence of market conditions, effort adjustments and management rules.

Our paper also contributes to a growing literature examining how keystone animal species influence economic outcomes (Alsan, 2015; Feir et al., 2024; Frank & Sudarshan, 2024). All these studies focus on the presence, disappearance, or local collapse of a single species of particular relevance, documenting effects on outcomes such as disease spread, agricultural production, occupational structure, and long-run economic development. In this paper we extend this literature by taking into account biological diversity across multiple species within the same ecosystem, while also considering their relevant ecological interactions. In our setting, diversity in fishes' thermal

preferences becomes a primary mediator of the impact of climate change on fisheries. To our knowledge, this is the first paper to incorporate this type of ecological complexity into empirical economic analysis.

The remainder of the paper is organized as follows. Section 2 describes the data sources and the construction of the MDD metrics. Section 3 introduces the theoretical framework that links SST to fishing revenue. Section 4 presents the empirical strategy. Section 5, 6, and 7 present the main results and the robustness checks. Section 8 provides projections under alternative climate scenarios. Section 9 concludes with policy implications and directions for future research.

2 Data

We construct a unique dataset by integrating information from several sources: fisheries revenue data from the Scientific, Technical, and Economic Committee for Fisheries (STECF) of the European Union, satellite SST data from the U.S. National Oceanic and Atmospheric Administration (NOAA) and data on fish species and ocean characteristics from different biological sources. We also get SST daily climate projections from the Earth System Model Version 4.1 (ESM4), developed by the Geophysical Fluid Dynamics Laboratory (GFDL) of NOAA. We provide a concise description of each data source below.

2.1 Fisheries revenue data

We use the spatial fishing dataset provided by the Scientific, Technical and Economic Committee for Fisheries (STECF) of the European Union. The dataset reports catches and *ex-vessel* revenue for all EU fishing vessels operating under the EU Common Fisheries Policy (CFP) over the period 2013-2022.

The EU CFP is the main framework governing fisheries management in EU waters and, operationally, aims to keep exploitation rates consistent with their Maximum Sustainable Yield (MSY), i.e., the largest long-run harvest that can be sustained without depleting the stock. The CFP measures are defined for each biological stock within a delineated management area: in other words, management is spatially explicit, and the relevant regulatory unit is a stock (species) inside a management area. Supplemental Appendix A.1 illustrates the type of management-area delineations observed in our data for an illustrative region (North Sea and Baltic Sea). These management areas align with Food and Agriculture Organization (FAO) fishing divisions and related statistical subdivisions.

In compliance with the reporting obligations under the CFP and the EU Data Collection Framework, each vessel must record the location of fishing activity, landed quantities by species, and the fishing technology and gear used. These trip-level records are compiled and harmonized in the STECF spatial product. Revenue is calculated using *ex-vessel prices*, i.e., the prices received by fishers at first sale when the catch enters the supply chain. A key feature of the STECF spatial data is that revenue is spatially geo-localized on the C-SQUARES grid (Concise Spatial QUery And REpresentation System), a global geocode system designed to enable simple spatial indexing of marine information (Rees, 2003). Grid cells have size $0.5^\circ \times 0.5^\circ$ (about 55 km at the equator), providing a very

fine resolution for the fisheries context.

Within each cell, observations are further disaggregated by species, vessel length class (e.g., 18-24 m), fishing technique (e.g., purse seine, bottom trawling) and fishing gear (e.g. trammel nets, boat dredges). Supplemental Appendix A.2, A.3 and A.4 provide the complete lists of vessel length classes, fishing techniques and gear types included in the dataset. On the biological dimension, the dataset covers a very broad range of species, including small pelagics (e.g., sardine, anchovy, mackerel), large pelagics (e.g., tunas), demersal finfish (e.g., cod, hake) and benthic organisms (e.g., cephalopods and crustaceans). While the raw data include more than 3,000 species and aquatic organisms, commercial value is concentrated in a relatively small subset. Consequently, we focus on the top 100 species (by value) which together account for about 95% of total revenue (Supplemental Appendix A.5 lists the included species). While these data are released with quarterly frequency, we aggregate them at the yearly level to abstract from within-year seasonality and align the analysis with the frequency of most management instruments.

Figure 1 presents the geographic distribution of the revenue data. The dataset includes fishing activity in both EU waters and non-EU Exclusive Economic Zones (EEZs).[1] This reflects the fact that EU fleets can operate beyond EU jurisdiction under bilateral agreements, such as reciprocal access. The dataset also includes fishing activity in international waters. EU overseas territories also generate limited observations in other ocean basins (e.g., Indian Ocean and Pacific Ocean) but, given their sparse nature (less than 4% of total revenue), we exclude them from the main analysis. Therefore, our baseline geographic domain includes all observations within FAO Major Fishing Areas 27 (North-East Atlantic), 21 (North-West Atlantic), 31 (Western Central Atlantic), 34 (Eastern Central Atlantic), 37 (Mediterranean and Black Sea), 41 (South-West Atlantic), and 47 (South-East Atlantic).[2]

[1] An EEZ is a sea region, extending up to 200 nautical miles (approximately 370 km) from a coastal state's baselines, within which the coastal state holds sovereign rights over the exploration and exploitation of marine resources, including fisheries.

[2] We perform several additional cleaning steps to address residual inconsistencies in the data. These procedures, documented in Supplemental Appendix A.6, affect less than 4% of the remaining observations. We also show that our main results are robust to these cleaning choices.

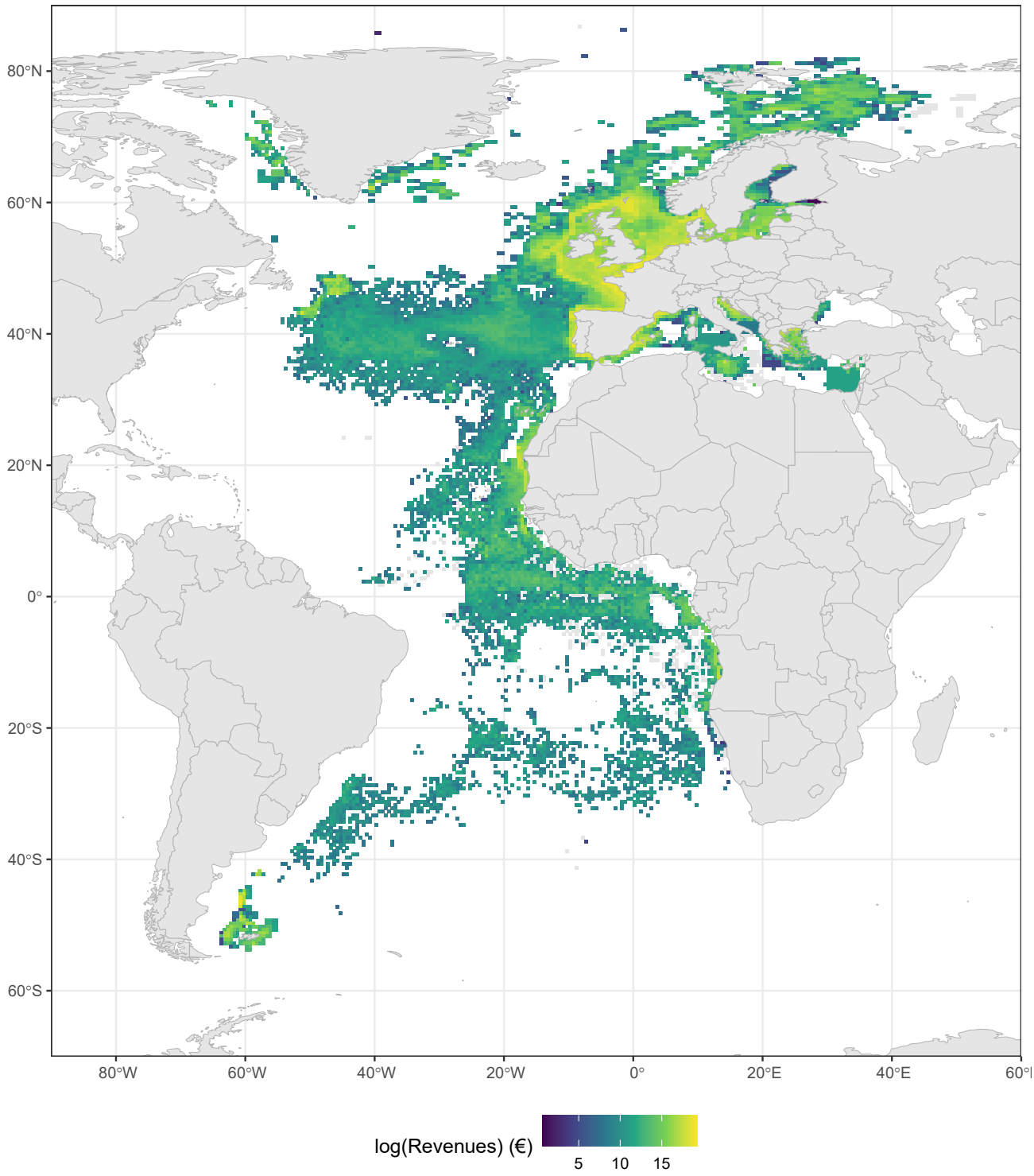


Figure 1: Spatial distribution of aggregate fishing revenue from the 100 most commercially important species, summed over the years 2013–2022, for EU vessels.

2.2 Sea surface temperature and thermal preferences

We measure ocean temperature using daily SST from the NOAA Optimum Interpolation Sea Surface Temperature (OISST) Analysis v2.1 (Huang et al., 2021). OISST provides global daily SST gridded data at the $0.25° \times 0.25°$ spatial resolution ($\sim 25km \times 25km$), calculated from satellite observations corrected with in situ measurements (ships, buoys, and Argo floats).

These data are available globally and constructed consistently over time. Our analysis employs daily temperature data for the 2013-2022 period, matching the time span of our fishing information.

To link temperature to fishing activity, we harmonize OISST data to the spatial resolution of our fishing dataset (c-square cells), calculating for each cell i and day d the relevant weighted average SST. Figure 2 presents the resulting variability in average SST across the FAO macro-areas in our sample, showing how mean temperature ranges differ substantially across areas. Our data effectively mirror the global spectrum of SST, encompassing temperatures from sub-zero conditions up to nearly 30°C. As expected, temperature is strongly related to latitude, and semi-enclosed basins (e.g. the Mediterranean) display a less variable distribution relative to open-ocean regions.

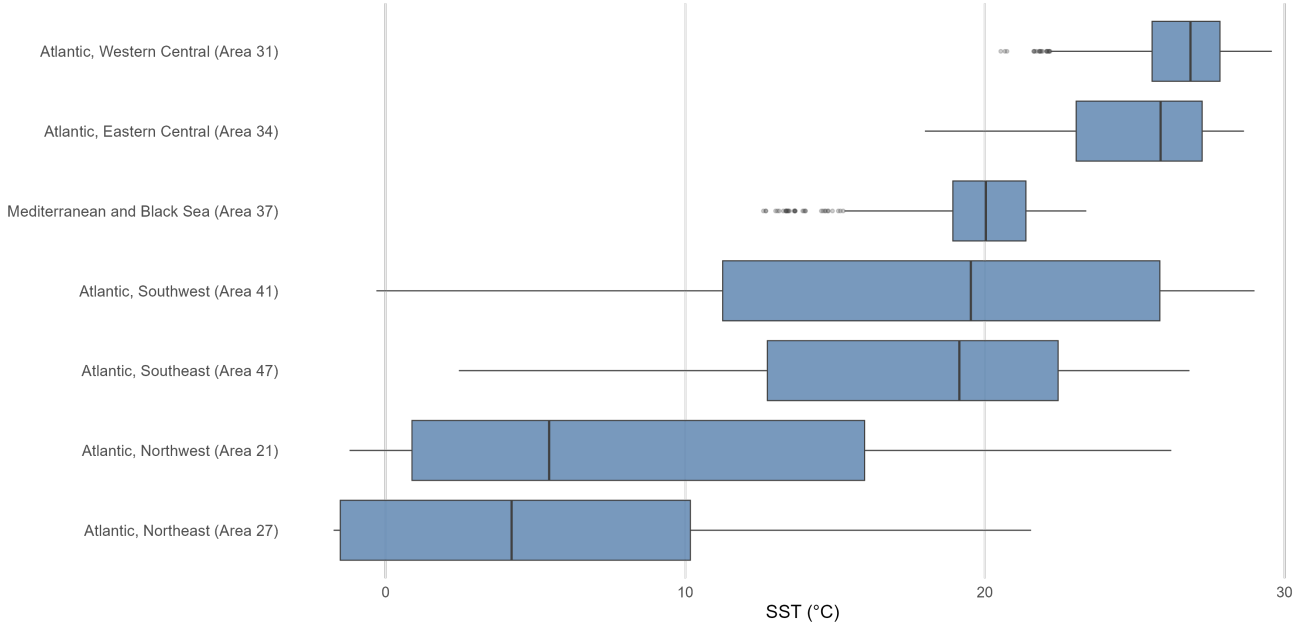


Figure 2: Distribution of the average SST (2013-2022) across the macro-regions (FAO areas) in our data.

We combine daily SST with species-level information on thermal preferences, defined as the SST range in which a species is typically found. Our main source of information is Cheung et al. (2013), which reports the interquartile range of SST preferences for more than 900 species of fish, shellfish, and crustaceans. For the five species in our sample not covered by Cheung et al. (2013), we use thermal ranges from FishBase (www.fishbase.org) and SeaLifeBase (www.sealifebase.org), two comprehensive and regularly updated repositories of biological information on marine species. These estimates rely on the AquaMaps framework, which combines occurrence records with ecological constraints from the literature to infer species-specific environmental envelopes, including temperature

tolerance bounds. Table A.6 in Supplemental Appendix A.5 reports the thermal range for each species included in the data.

It is worth noting that, although fish inhabit various depths of the water column and, therefore, experience temperatures that differ from our SST, this does not pose a problem for our analysis for two key reasons. First, thermal preferences are already expressed in terms of SST, thereby inherently accounting for depth-related temperature gradients. Second, the cell-specific day-to-day variability of SST is highly correlated with the corresponding temperature variability in the deeper ocean layers (see Supplemental Appendix A.7, which compares SST variation against daily bottom sea temperature). Given that our model controls for location-specific characteristics, the strong within-location covariance between SST and deeper-water temperatures supports the use of SST as our thermal exposure measure.

In order to represent species' different exposure to the same temperature we use MDDs, which employ the same logic of the degree-day measures widely used in agricultural and energy economics (Hogan & Schlenker, 2024). Degree-days measure aggregate daily deviations from biologically or behaviorally relevant thresholds into a cumulative indicator that captures both the intensity and the duration of thermal conditions[3]. Our two MDD metrics are constructed in an analogous way, i.e. by summing daily deviations from species-specific thermal bounds, yielding two annual exposure indexes. Since we want to identify both the effect of temperature below and above the thermal preference, we separately compute the cold exposure and the heat exposure as:

$$MDD_{is}^{+} = \sum_{d=1}^{365} (SST_{id} - TP_s^{max}) \cdot \mathbb{1}(SST_{id} > TP_s^{max}) \tag{1}$$

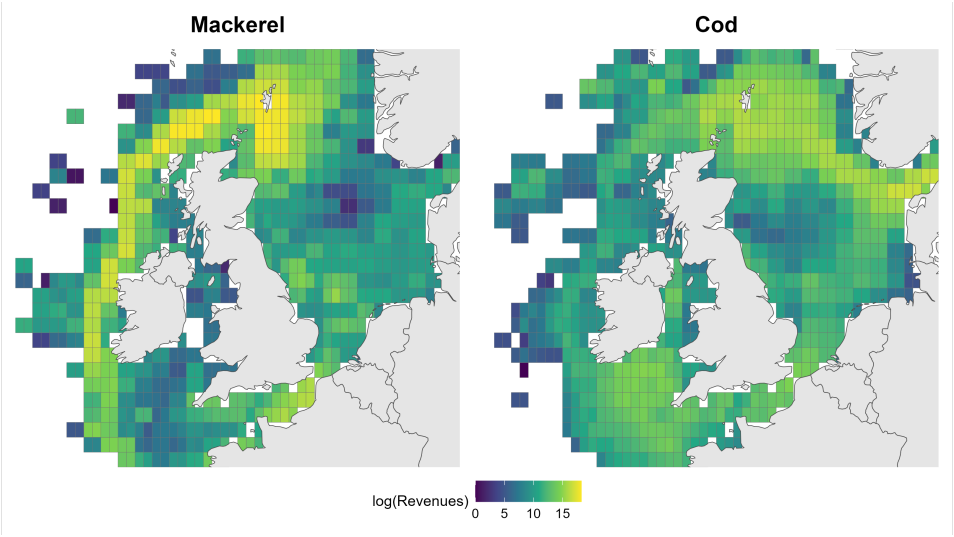
$$MDD_{is}^{-} = \sum_{d=1}^{365} (TP_s^{min} - SST_{id}) \cdot \mathbb{1}(SST_{id} < TP_s^{min}), \tag{2}$$

where SST_{id} is the SST on day d at location i, and TP_s^{min} and TP_s^{max} denote the lower and upper bounds of the preferred thermal interval for species s.

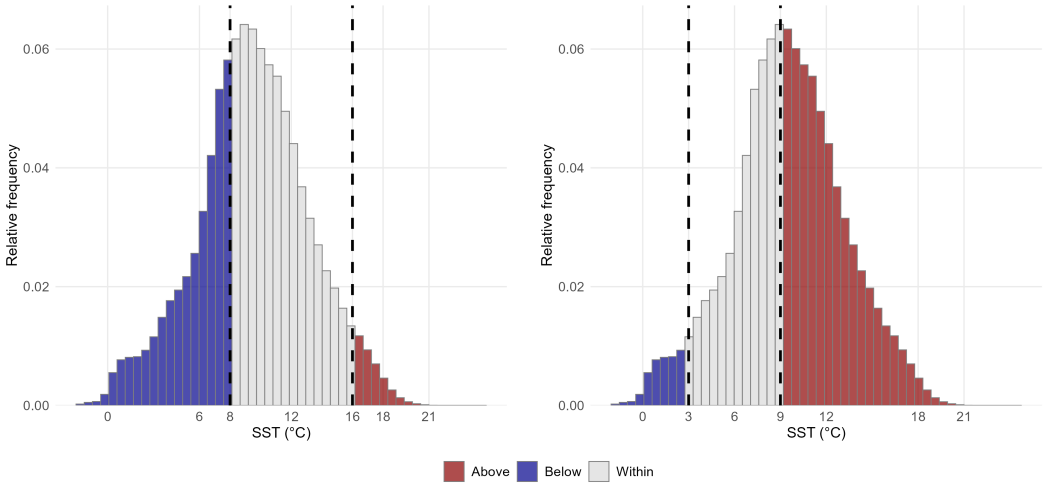
Figure 3 illustrates how the interaction between variation in temperature and in species' thermal tolerances generates differences in exposure. The left column of the figure refers to the Atlantic mackerel, while the right column refers to the Atlantic cod. These two high-value species both live in the North Sea, but exhibit different thermal preferences. Panel 3a maps the distribution of the log of revenue for the two species. Panel 3b shows the distribution of SST in this region, comparing it with the thermal tolerance bounds for the two species. The histograms show that the same underlying temperature distribution can translate into markedly different exposure profiles across species, even for overlapping locations. Panel 3c provides a visual summary of the resulting heterogeneity, showing how heat exposure (MDD+) can markedly differ across both space and species. In this specific case, even if the

[3]For example, in energy economics, heating (or cooling) degree days are widely used to quantify energy demand. They are computed relative to a reference temperature, interpreted as the threshold below (or above) which households typically begin heating (or cooling) their homes (Fowlie et al., 2018). In agriculture and ecology, growing degree days are an analogous concept used to measure cumulative heat exposure relevant for the biological growth and development of a crop (Schlenker et al., 2006).

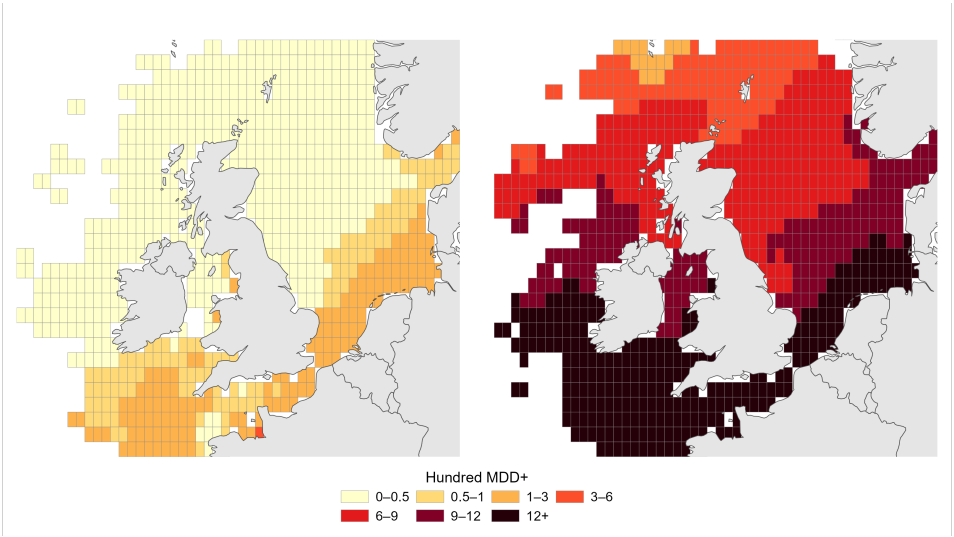
two species are exposed to the same ocean temperatures, mackerel exhibits substantially less heat stress than cod because its thermal preference is skewed toward warmer waters. This cross-species, within-location variation in exposure is the main source of variation that we exploit in the empirical analysis.



(a)



(b)



(c)

Figure 3: Panel (a) shows the revenue distribution for two key commercial species, the Atlantic mackerel and the Atlantic cod across the same area summed over the full period 2013-2022. Panel (b) shows the distribution of temperature across the same region together with the different thermal range the two species have. Panel (c) shows the heat exposure (MDD+) for the two species for an average year in our dataset.

2.3 Additional biological and environmental data

We obtain additional species-level characteristics from FishBase and SeaLifeBase. Specifically, we collect information on species depth ranges, ecological categories, resilience, and migratory behavior. We use these variables to inform our heterogeneity and robustness analyses.

We also obtain information on ecological interactions among species from Ecopath with Ecosim, an open-source software platform for modeling marine ecosystems (Christensen & Walters, 2004). In particular, we use Mixed Trophic Impact matrices for the Mediterranean and Atlantic ecosystems, based respectively on Piroddi et al. (2015) and Palomares and Pauly (2014). These matrices summarize the direct and indirect trophic effects of one species on another. Their construction and use are described in Section 4.3 and Supplemental Appendix B.

Finally, we obtain spatial information on ocean characteristics from Bio-ORACLE, an open-access database widely used in marine ecological applications (Assis et al., 2024). Specifically, we use bathymetry (depth), seabed rugosity, surface salinity, and bottom salinity.

2.4 Climate change projections data

In order to simulate the impact of future climate changes on fishing revenue, we use daily SST projections under alternative climate-change scenarios from the Earth System Model version 4.1 (ESM4.1), developed by NOAA's Geophysical Fluid Dynamics Laboratory (Dunne et al., 2020). ESM4.1 is a coupled chemistry-carbon-climate model designed for comprehensive Earth-system simulations and provides daily projected SST at a spatial resolution of $1^\circ \times 1^\circ$ over the period 2015-2100. In the main projection exercise, we focus on two Shared Socioeconomic Pathways (SSPs), SSP-2.45 and SSP-3.70. These scenarios were included among the Tier 1 experiments in CMIP6 (Tebaldi et al., 2021) and represent intermediate-to-high, but non-extreme, emissions pathways. This choice is motivated by the recent discussion among climate scientists, which emphasizes a narrower range of policy-relevant and plausible future emissions trajectories than the full CMIP6 scenario envelope (Van Vuuren et al., 2026). The numerical labels refer to the approximate radiative forcing level reached by 2100. Thus, SSP-2.45 represents a lower-emissions trajectory than SSP-3.70. For details on the SSP scenarios, see Riahi et al. (2017).

3 Theoretical model

This section develops a stylized theoretical model showing how changes in temperature can affect fishing revenue via changes in biological productivity. To keep the exposition transparent and avoid heavy notation, we present a non-spatial formulation for a single species. Supplemental Appendix C extends the framework to allow for biomass adjustments across neighboring areas and ecological interactions across species.

We begin with the ecological dynamics. Fish biomass at time $t+1$ is given by biomass at time t plus net growth between t and $t+1$:

$$B_{t+1} = B_t + G(B_t, K_t, r) - h(B_t, E_t, q), \tag{3}$$

where $G(\cdot)$ is biological growth, which depends on current biomass B_t, the carrying capacity of the environment K_t, and the intrinsic growth rate r, a species-specific biological parameter capturing its inherent capacity to reproduce (Froese et al., 2017). The carrying capacity summarizes the maximum biomass the habitat can sustain while still allowing positive net growth, and has a time subscript because we will allow it to be affected by ocean temperature. Harvest $h(\cdot)$ depends on biomass abundance, fishing effort E_t, and a catchability parameter q.

Trivially, the change in biomass between two consecutive periods can be written as:

$$\Delta B_t = G(B_t, K_t, r) - h(B_t, E_t, q). \tag{4}$$

Following the Gordon-Schaefer model (Gordon, 1954), we specify a logistic growth function as:

$$G(B_t, K_t, r) = r \cdot B_t \cdot \left(1 - \frac{B_t}{K_t}\right). \tag{5}$$

This expression implies an inverse U-shaped relationship between population growth and biomass (Figure 4, left panel). When biomass is low, growth is limited by the small stock size even if ecological resources are abundant. When biomass is high, density-dependent constraints reduce net growth despite the large stock. The carrying capacity K_t is the biomass level at which net growth becomes zero.

Within the same Gordon–Schaefer framework, we define the harvest production function as:

$$h(B_t, E_t, q) = q \cdot E_t \cdot B_t, \tag{6}$$

where the catchability coefficient q represents the fraction of the stock harvested per unit of effort and is determined by both the species characteristics and fishing technologies.

Substituting (5) and (6) into (4) yields:

$$\Delta B_t = r \cdot B_t \left(1 - \frac{B_t}{K_t}\right) - q \cdot E_t \cdot B_t. \tag{7}$$

A classic challenge in empirical fisheries research is that B_t is not directly observed. To overcome this issue, we introduce a simple equilibrium concept motivated by the CFP management objectives. The CFP governs fisheries management in the areas of our analysis, and has the objective to ensure that the "fish stock management [is] at maximum sustainable yield for all managed stocks". We interpret this objective as the regulator's target. Under our biological model, the biomass stock associated with maximum sustainable yield equals half of the carrying capacity[4]:

[4]Supplemental Appendix C presents a formulation of the model with a less strict equilibrium assumption, while the equation

$$B_t^{MSY} = \frac{K_t}{2}. \tag{8}$$

Even well-intentioned managers cannot perfectly achieve a biological target. To represent the objective, and the error in achieving it, we introduce a stochastic component that allows biomass stock to deviate from this target. We assume biomass to be:

$$B_t = \frac{K_t}{2} \cdot exp(\varepsilon_t), \tag{9}$$

where ε_t is a zero-mean normally distributed random variable. This assumption suggests that observed biomass at any given time will be "near" the management target of $\frac{K_t}{2}$. It also recognizes that changes in K_t over time (which, in our model, will be driven by changes in ocean temperature and other characteristics), can affect the target (and the realized) biomass.

Regarding the effect of temperature on fisheries, we follow Barbier (2000), and assume that temperature affects habitat productivity, which affects the carrying capacity of the fish stock. We denote the realization of the distribution of ocean temperature in year t by τ (as explained in the previous section, our empirical model represents it in terms of MDDs). We treat temperature as a realization of an underlying climate distribution and, therefore, as unaffected by fishing activity (Hsiang, 2016).

Specifically, we assume:

$$K_t(\tau_t, \chi) = f(\tau_t) \cdot g(\chi_t), \tag{10}$$

where $f(\tau_t)$ is a temperature-response function for the species in question and χ_t captures all non-temperature features of the habitat such as depth, seabed ruggedness, upwelling dynamics and ocean currents. The function $g(\cdot)$ maps these habitat characteristics into the non-temperature component of carrying capacity.

Because K_t enters the growth function, changes in τ_t shift the entire growth function. In our biological model, a larger value of K_t increases both $G(\cdot)$ and B_t. Therefore, in our model there is a single temperature realization that produces the maximum value of K_t: we refer to this temperature as the "optimal" temperature for that species. When temperature is either above or below that optimum, growth is lower. This is illustrated in Figure 4, where the left panel presents the growth function under a hypothetical optimal temperature (18°C), and the right panel shows growth under a different, in this case higher, temperature (22°C).

We substitute (10) and (9) into the harvest function (6), giving:

$$h_t = f(\tau_t) \cdot g(\chi_t) \cdot q \cdot E_t \cdot \frac{exp(\varepsilon_t)}{2}. \tag{11}$$

supporting the empirical model remains almost identical.

Multiplying by price, p_t, gives revenue R_t as:

$$R_t = p_t \cdot f(\tau_t) \cdot g(\chi_t) \cdot q \cdot E_t \cdot \frac{exp(\varepsilon_t)}{2}. \tag{12}$$

Taking logs provides the foundation for our empirical models:

$$\log(R_t) = f^*(\tau_t) + g^*(\chi_t) + \log(q) + \log(E_t) + \log(p_t) + \varepsilon_t - log(2), \tag{13}$$

where $f^*(\tau_t) \equiv \log(f(\tau_t))$ and $g^*(\chi_t) \equiv \log(g(\chi_t))$. Equation 13 illustrates the causal effect of temperature on fishing revenue, which is the central relationship of interest in our study.

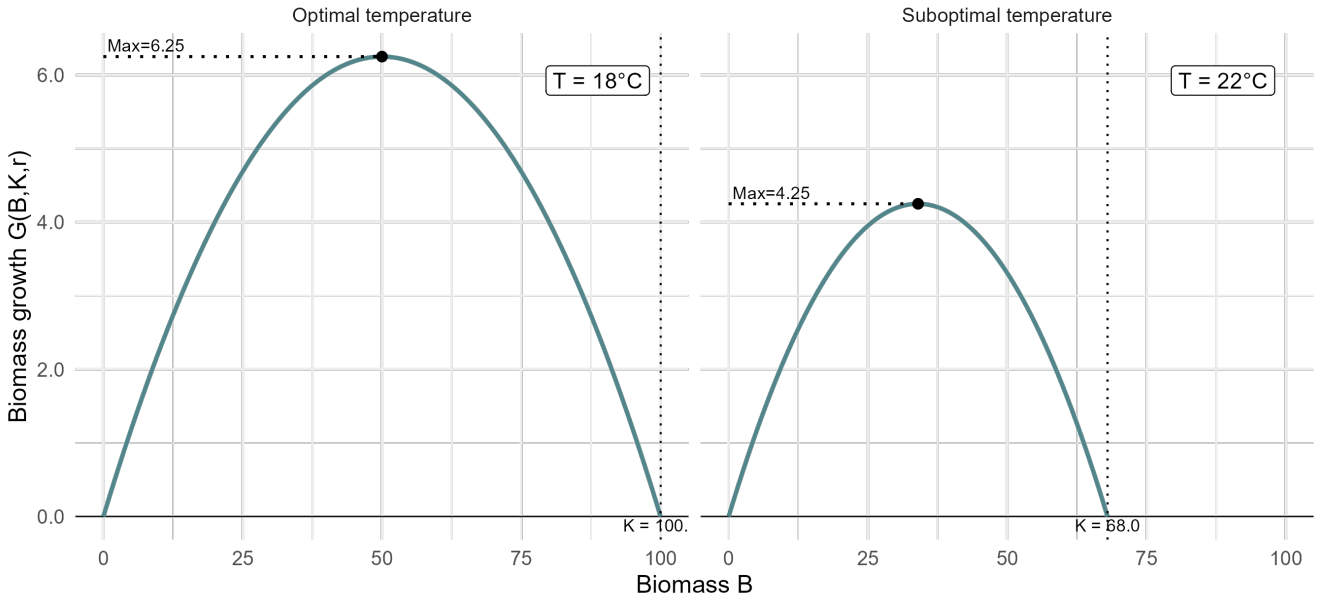


Figure 4: Biomass growth under hypothetical optimal (left) and suboptimal (right) temperatures. Parameter values are illustrative.

4 Empirical specification

This section starts by illustrating our baseline specification, which we then extend to take into account different additional features such as species-specific habitats, trophic interactions and sample selection. We report all these model extensions in the main results section, and then carry out a full set of robustness tests and consider further issues such as non-linear heterogeneous effects in the following sections.

4.1 Baseline model

Our baseline model builds on the existing climate change economics literature (Hogan & Schlenker, 2024) by specifying the effect of temperature as a linear function of MDD^+ and MDD^-. Considering the species s in cell i in year t, we write:

$$f^*(\tau_{its}) = \beta_1 * MDD^-_{its} + \beta_2 * MDD^+_{its} \tag{14}$$

The parameters β_1 and β_2 reflect the marginal (log) revenue response to cold and heat exposure. This functional form has two important features. First, because MDD^+ and MDD^- are measured relative to each species' thermal preferences, this approach is able to identify the heterogeneous impact of temperature changes on each species. Second, it allows for the estimation of different impacts for temperatures colder and warmer than the preferred thermal range.

In order to derive our revenue equation, we also introduce: (1) a technology index j, defined as the interaction between vessel length class, fishing technique, and gear type; and (2) a management-area index l. Our baseline empirical specification is, therefore:

$$log(R_{itsj}) = \beta_1 \cdot MDD^-_{its} + \beta_2 \cdot MDD^+_{its} + \alpha_{itj} + \gamma_{stlj} + \xi_{itsj} \tag{15}$$

where R_{itsj} is the fishing revenue in year t, cell i, from species s caught with technology j. This specification includes two high-dimensional fixed effects: α_{itj} is a cell-by-year-by-technology fixed effect, and γ_{stlj} is a species-by-year-by-management-area-by-technology fixed effect. Finally, ξ_{itsj} is the stochastic error term.

The term α_{itj} absorbs all determinants of revenue that are common to all species caught in the same cell i, year t, and technology j. Its main function is to absorb both the spatial selection into fishing locations and the fishing effort deployed in cell i in year t with technology j (the biological aspect of selection, i.e. the fact that a species can be caught or not in a given cell-year, is explored in section 6.1). Furthermore, it controls for all cell-by-time omitted variables that affect revenue through channels other than the species-specific thermal exposure embedded in MDD^+ and MDD^-. This includes time varying local conditions such as short run ocean productivity and ecosystem states (e.g., plankton blooms, oxygenation), local weather that affects fishing feasibility, local pollution and temporary spatial restrictions (closures, marine protected areas, conflict with other maritime uses).

The term γ_{stlj} absorbs all shocks that are specific to species s in management area l and year t, for a given technology j. This is the natural level at which both market conditions and fisheries management are defined and, therefore, it removes three important omitted variables. First, it controls for species-specific market conditions, such as prices, at the relevant spatial scale, since catches within the same management area are typically marketed through the same landing ports and supply chains. Second, it also captures other persistent or slow-moving determinants of species' specific revenue, such as differences in average catchability of a species, evolution in targeting ability

for each given technology, area-specific monitoring/enforcement intensity, and institutional features that can vary across management areas and fleet segments. Finally, it absorbs species-specific biological or ecological shocks occurring at the management-area level that may affect stock abundance and that are not under the control of the manager, such as changes in upwelling and primary productivity, or episodes of mass mortality.

With α_{itj} and γ_{stlj} included, the coefficients β_1 and β_2 are identified from residual variation in thermal exposure that 1) varies among different species within the same cell year and technology, 2) varies among cells within the same management area, for the same species, year and technology. The first source of variation arises when species with different thermal preferences are caught in the same cell, since they will experience different MDD^+ and MDD^- levels. The second one simply exploits the cross-sectional changes in thermal exposure for the same species within a management-area. The next sections extend this baseline specification in several directions.

4.2 Habitat suitability

We now modify our baseline specification to take into account that time-invariant cell characteristics may generate species-specific suitability patterns that can be potentially correlated with differences in thermal exposure. For example, bathymetry and seabed ruggedness can affect local habitat quality and species composition. If these characteristics are correlated with SST variation within a management area, our results could be affected by omitted variable bias. In our setting we cannot include species-by-cell fixed effects, since they would absorb nearly all of the relevant identifying variation in thermal exposure, as shown in Supplemental Appendix D.1. Therefore, we include two different sets of coefficients in order to control for changes in species-specific habitats across cells and, at the same time, retain our main source of identifying variation.

First, we augment the baseline model by including interaction effects between species fixed effects and cell characteristics. Specifically, we interact measures of cell bathymetry, terrain rugosity, surface salinity, and bottom salinity with species indicators, allowing the relationship between local habitat characteristics and revenue to differ across species. We obtain these cell characteristics from Bio-ORACLE (Assis et al., 2024).[5]

Second, we account for unobserved spatial patterns that may differ between species. To do so we interact species indicators with the basis functions of a two-dimensional thin-plate spline in latitude and longitude. This approach follows the logic as in Dell (2010), which uses flexible functions of latitude and longitude to absorb unobserved spatial heterogeneity.

We define:

$$h_s(\text{lat}_i, \text{lon}_i) = \sum_{k=1}^{K} \omega_{sk} B_k(\text{lat}_i, \text{lon}_i),$$

where $B_k(\text{lat}_i, \text{lon}_i)$ are spline basis functions and the coefficients ω_{sk} are allowed to differ by species. This allows

[5]Bio-ORACLE also provides variables such as dissolved oxygen, chlorophyll, and other chemical or productivity-related measures. We do not include these variables in the model because they are causally affected by temperature and therefore act as bad controls (Angrist & Pischke, 2008).

each species to have its own smooth spatial suitability gradient. These gradients can capture broad spatial features of the marine environment that are not (fully) captured by the fixed effects, such as large-scale ocean circulation, upwelling systems, proximity to productive fronts or the shape and width of the continental shelf.

Combining these controls with the baseline specification gives:

$$\log(R_{itsj}) = \beta_1 MDD^{-}_{its} + \beta_2 MDD^{+}_{its} + \alpha_{itj} + \gamma_{stlj} + \sum_m \phi_{sm} Z_{im} + h_s(\text{lat}_i, \text{lon}_i) + \xi_{itsj}. \tag{16}$$

where Z_{im} denotes the set of observed cell characteristics from Bio-ORACLE, and the coefficients ϕ_{sm} are species-specific slopes.

4.3 Trophic interactions

Thermal exposure may affect a species not only through its own biology, but also indirectly through changes in the local fish stock. In fact, marine species interact by preying on one another or competing for the same resources. In ecology, these interdependencies are referred to as trophic interactions, i.e. the feeding relationships through which energy flows between species (Kaiser, Michel J. et al., 2020).

Trophic interactions could alter the carrying capacity (and hence the revenue) of each species. Because temperature can alter both species' abundances and interaction strengths (Durant et al., 2019), a temperature shock may generate spillovers across trophically linked species. For example, warming may reduce the biomass of a predator (or competitor) of a species, indirectly improving its carrying capacity and revenue even if such species is not affected directly[6]. This interference would constitute a violation of the Stable Unit Treatment Value Assumption (SUTVA), because the outcome of the species would depend not only on its own thermal exposure, but also on the exposure experienced by trophically connected species.

To account for these indirect effects, we construct an original index that summarizes the thermal exposure of the trophic network of each species. We call this index *Heat Exposure of Aquatic Trophic Exchanges* (HEATEX). Conceptually, HEATEX measures the average exposure of the other species in the same cell-year to temperatures above or below their own preferred range, weighting each species by its trophic relevance for species s. Such relevance is expressed by the mean of *trophic weights* that are derived from the *mixed trophic impact* (MTI) approach widely used in marine ecology, which can be interpreted as the ecological analogue of a Leontief input-output matrix, with species or functional groups replacing economic sectors (Ulanowicz & Puccia, 1990). Supplemental Appendix B reports the formal definition of the index, the data sources, and additional implementation details.

We compute the index separately for the exposure below and above the thermal preferences of the interacting species and we represent them as H^{-}_{its} and H^{+}_{its} respectively. Including the two terms in equation 16 we obtain:

[6]Supplemental Appendix C formalizes why, in such settings, the outcome of the species s can depend on the thermal exposure experienced by other species in the community.

$$\log(R_{itsj}) = \beta_1 \cdot MDD^-_{its} + \beta_2 \cdot MDD^+_{its} + \theta^- \cdot H^-_{its} + \theta^+ \cdot H^+_{its} + \alpha_{itj} + \gamma_{stlj} + \sum_m \phi_{sm} Z_{im} + h_s(\text{lat}_i, \text{lon}_i) + \xi_{itsj}. \tag{17}$$

Including H^-_{its} and H^+_{its} provides a way to net out temperature-driven changes in the trophic environment that could otherwise be absorbed into the estimated response of species s to its own exposure, and the coefficients θ^- and θ^+ capture whether revenue for species s is affected by cold or heat stress experienced by trophically connected species.

5 Main results

Table 1 reports our main estimates. Coefficients are reported multiplied by 100, so that they represent the semi-elasticity of fisheries revenue with respect to a variation of 100 MDD. Standard errors are clustered at the cell level. Supplemental Appendix D.2 reports the results under alternative clustering choices.

Our baseline specification is reported in the first column of the table. Both coefficients are negative and highly significant, indicating that departures from species' preferred temperatures reduce fishing revenue. The effect of heat exposure is substantially larger in magnitude: a hundred-unit increase in MDD^+ decreases revenue by about 15%, while an equivalent increase in MDD^- leads only to a 4.7% reduction.

To provide a sense of magnitude, consider Atlantic mackerel, the species generating the highest aggregate revenue in our sample, i.e. approximately €332 million yearly. Averaging across its full geographical range, in our dataset the mean annual heat exposure is approximately 320 MDD^+. A 15% increase in heat exposure (approximately 50 additional MDD^+), consistent with SSP-3.70 climate change scenario projections for years 2050-2075, would reduce annual revenue by about 7.2%. This corresponds to a loss of around €24 million per year.

Column (2) augments the baseline specification with the two sets of species-specific parameters designed to account for differences in habitat suitability as explained in section 4.2. These controls absorb both observed habitat characteristics and remaining smooth spatial differences in species-specific suitability.

In this specification the coefficients remain negative, statistically significant, and within the 95% confidence intervals of the baseline model. This result suggests that the baseline specification is robust to the inclusion of species-specific habitat suitability and spatial gradients.

In column (3) we add to the previous model the HEATEX controls (also multiplied by 100 to improve readability), in order to account for temperature-induced ecological spillovers through trophic interactions. We call this specification the "full model" and, in the rest of the paper, we will use it as the reference specification for robustness testing and heterogeneity analysis. Again, the coefficients on MDD^+ and MDD^- remain similar to those in Column (1), indicating that the estimated effect of a species' own thermal exposure is not strongly affected by omitted exposure of trophically connected species. In other words, even after explicitly controlling for the thermal stress experienced by the local trophic network, the direct effect of the species' own exposure on its revenue remains the

dominant relationship in the data. However, the HEATEX coefficients themselves suggest that trophic exposure matters. In fact, the negative and statistically significant coefficient of H^+ implies that when the beneficial species are harmed by high temperatures, the revenue of the focal species also declines (see Supplemental Appendix B for details). The coefficient on H^- points in the same direction, but is smaller in magnitude, mirroring the main findings on the direct exposure. Heat exposure seems to be the dominant source of damage, both directly and, to a lesser extent, indirectly through the trophic network.

Table 1: Main estimation results and robustness to alternative specifications

Dependent variable:	log(Revenue)		
Model:	Baseline model	Species-specific controls	Full model
	(1)	(2)	(3)
Thermal exposure			
MDD^+ ($\times 100$)	-0.153^{***}	-0.131^{***}	-0.132^{***}
	(0.013)	(0.012)	(0.013)
MDD^- ($\times 100$)	-0.047^{***}	-0.038^{***}	-0.044^{***}
	(0.009)	(0.011)	(0.012)
Trophic-interaction controls			
H^+ ($\times 100$)			-0.011^{***}
			(0.003)
H^- ($\times 100$)			-0.003^{***}
			(0.001)
Fixed effects			
α_{itj}	Yes	Yes	Yes
γ_{stlj}	Yes	Yes	Yes
Species-specific controls			
Habitat characteristics	No	Yes	Yes
Smooth spatial gradients	No	Yes	Yes
Fit statistics			
Observations (millions)	2.542	2.542	2.542
R^2	0.84	0.84	0.84

Notes: Standard errors clustered at the cell level are reported in parentheses.
Habitat characteristics include bathymetry, terrain, surface and bottom salinity.
Smooth spatial gradients are species-specific slopes in spline functions of latitude and longitude.
H^- and H^+ denote HEATEX controls for cold and hot exposure of trophically connected species.
Significance levels: $^{***}p < 0.01$, $^{**}p < 0.05$, $^{*}p < 0.1$.

6 Robustness tests

6.1 Sample selection

The dataset reports revenue only for species that are actually caught, so zero revenue is not observed. This clearly raises an issue of sample selection. However, it is useful to distinguish between two forms of selection. The first is a *fisher-driven selection*: vessels decide where, when, and how to fish. This margin operates at the cell-year-technology level and is completely controlled for by our fixed effect α_{itj}. The second is a *biological selection*:

conditional on fishing taking place in cell i, year t, and technology j, some species that could plausibly be caught with that technology in that area may not appear in the landings.

In order to also control for the second form of selection, we construct a comprehensive set of *implicit zeros*. For every cell-year-technology combination with fishing activity, we identify all the species that are feasible to catch with that technology in the same management area. We classify a species as "feasible to catch" with a certain technology when it is caught at least once in the same management area during the entire time span covered by our data with that technology. When a "feasible to catch" species is absent from a particular cell-year-technology combination, we generate an observation with zero revenue. Following this approach we identify approximately 1.8 million implicit zeros and add them to the original dataset.

To replicate the full-model specification on the augmented dataset, we must determine how to treat zero-revenue observations. The issue is twofold: 1) the logarithm is undefined at zero, and 2) applying ordinary least squares (OLS) to data with a large number of censored observations leads to biased estimates (Amemiya, 1984; Tobin, 1958). A common solution is to use transformations such as $\log(1+y)$ or the inverse hyperbolic sine. However, as recently discussed by Chen and Roth (2024), these transformations make the estimates depend on the scale of the dependent variable, thereby complicating the usual semi-elasticity interpretation.[7]

Following the discussion in Chen and Roth (2024) we implement two different strategies. First, we use a calibrated log transformation that retains the standard logarithmic transformation for positive revenues and assigns the zero-revenue observations a fixed negative value. Formally, we define:

$$m_x(R_{itsj}) = \begin{cases} \log(\max(R_{itsj}, 1)), & R_{itsj} > 0, \\ -x, & R_{itsj} = 0. \end{cases}$$

The parameter x determines the weight placed on the extensive margin, namely the transition from a species being absent from the landings to generating positive revenue. The advantage of this approach is that this weight is chosen explicitly rather than being implicitly determined by the scale of the dependent variable. Our preferred calibration sets $x = 1$, assigning zero-revenue observations a value of -1 and thereby placing an explicit weight of one log point on the extensive margin. Supplemental Appendix D.3.2 provides a more formal interpretation of this calibration and shows that the results remain stable across a wide range of alternative values of x.

As an alternative strategy, we estimate our model using a Poisson Quasi-Maximum Likelihood (PQML) regression, which extends the established Poisson regression by allowing the variance of the distribution to differ from its mean. This approach naturally accommodates zero outcomes and preserves the semi-elasticity interpretation of the coefficient (Wooldridge, 2002). However, as emphasized by Chen and Roth (2024), the PQML models the conditional mean in levels and, therefore, can place disproportionate influence on observations in the extreme upper tail of the outcome distribution, making it very sensitive to large outliers. To reduce such sensitivity of our estimates to

[7] The issue can be summarized as follows: adding 1 to the dependent variable implicitly assigns a specific value to the transition from zero to a positive outcome on the transformed log scale. This value depends on the unit in which the outcome is measured, for example euros rather than thousands or millions of euros, and therefore determines the implicit weight placed on the extensive margin.

a small number of exceptionally large revenues, we exclude the top 0.5% of revenue observations. Supplemental Appendix D.3.1 reports the complete set of PQML estimates and examines their sensitivity to alternative treatments of the upper tail.

Table 2 compares the full model with the calibrated-log and PQML specifications estimated on the augmented sample. The estimates remain remarkably similar across approaches, indicating that our main results are not affected by biological selection into observed landings.

Table 2: Robustness to implicit zero-revenue observations

Model:	Full model	Calibrated log	PQML
Dependent variable:	log(Revenue)	m_1(Revenue)	Revenue
Thermal exposure			
MDD^+ ($\times 100$)	-0.132^{***}	-0.123^{***}	-0.133^{***}
	(0.013)	(0.014)	(0.015)
MDD^- ($\times 100$)	-0.044^{***}	-0.032^{***}	-0.052^{***}
	(0.012)	(0.012)	(0.015)
Fit statistics			
Observations (millions)	2.542	4.386	4.364
$(Pseudo)R^2$	0.84	0.78	0.89

Notes: Standard errors clustered at the cell level are reported in parentheses. All specifications include trophic-interaction controls, species-specific slopes for habitat characteristics, and smooth species-specific spatial gradients. Significance levels: $^{***}p < 0.01$, $^{**}p < 0.05$, $^{*}p < 0.1$.

6.2 Spatial spillovers

Marine ecology suggests that temperature fluctuations can alter the spatial distribution of fish species (Auth et al., 2018). In our setting, this raises a possible criticism: a temperature shock could reduce revenue in one cell but increase revenue in nearby cells if fish move across space. Such displacement could generate spatial spillovers that could affect our causal estimates because of SUTVA violation.

However, theoretical considerations suggest that potential spatial spillovers should not affect our estimates. According to our stylized model, in fact, any movement of fish from one cell to another would lead to a decrease in biomass growth in the receiving cell due to an increase in ecological competition. Therefore, if management aims at maintaining the maximum sustainable yield locally, temperature still affects revenue primarily through changes in local habitat suitability (carrying capacity), rather than through persistent reallocation of biomass across neighboring cells (Supplemental Appendix C formalizes this argument). However, fisheries management operates at the management-area level rather than at the individual cell level, so that redistribution of biomass within management areas may still affect our estimates. Therefore, it is worth assessing whether our estimates are sensitive to potential spatial reallocation of the biomass.

We test this by re-estimating the full model (Table 1 column 3) after progressively aggregating the spatial grid. If temperature shocks mainly affect revenue by reallocating fish across neighboring cells, then aggregating neighboring cells should internalize this displacement as losses in one cell and gains in the nearby cells would offset

each other. The main model uses 0.5°×0.5° cells, corresponding to approximately 55×55 km at the equator. We then coarsen the grid to 1°×1° cells (110×110 km), and to 2°×2° cells (220×220 km). For each aggregation level, we sum revenue within the new spatial unit and recompute thermal exposure by averaging daily SST realizations over the same area.

We also present our results after aggregating cells at the management-area level. This specification differs from the finer-scale models in two ways. First, because the unit of observation is now defined at the management-area level, we can no longer include the same species-by-year-by-management-area-by-technology fixed effects used in the baseline. We therefore replace the management-area level fixed effects with FAO-major-areas fixed effects. Second, aggregation reduces the number of spatial units to only 143 management areas, with an average size of approximately 160,000 km^2. At this level of aggregation, the flexible species-specific spatial spline used in the preferred specification is no longer appropriate. We therefore retain only species-specific coefficients for the environmental characteristics of each management area.

Table 3 reports the results. Across the 1° and 2° grids, the estimates remain negative and statistically significant for both MDD^+ and MDD^-. Moreover, the 0.5° model point estimates fall within the confidence intervals of the estimates obtained using more aggregated spatial units. At the management-area level, the point estimates differ from the 0.5° ones, and are accompanied by wider confidence intervals. This is expected: aggregating to management areas sharply reduces the number of spatial units and absorbs much of the within-area variation used for identification. Nevertheless, the same pattern of heat exposure having the largest effect (in absolute value) is preserved. Furthermore, the confidence intervals from this model still include the main model's estimates. Overall, the stability of both the sign and the magnitude of the estimates across aggregation levels is reassuring. It suggests that the baseline results are not affected by biomass spillovers across neighboring cells.

Table 3: Robustness to alternative spatial aggregation

Dependent variable:	log(Revenue)			
Spatial grid:	0.5° × 0.5°	1° × 1°	2° × 2°	Management area
	(1)	(2)	(3)	(4)
Thermal exposure				
MDD^+ (×100)	-0.132^{***}	-0.136^{***}	-0.168^{***}	-0.209^{***}
	(0.013)	(0.020)	(0.037)	(0.051)
MDD^- (×100)	-0.044^{***}	-0.054^{***}	-0.058^{***}	-0.107^{**}
	(0.012)	(0.017)	(0.016)	(0.044)
Fit statistics				
Observations (millions)	2.542	1.208	0.709	0.403
R^2	0.84	0.78	0.78	0.81

Notes: Standard errors clustered at the cell level are reported in parentheses. All specifications include trophic-interaction controls, species-specific slopes for habitat characteristics. All the specifications, excluding the management areas aggregation also include smooth species-specific spatial gradients. Significance levels: $^{***}p < 0.01$, $^{**}p < 0.05$, $^{*}p < 0.1$.

6.3 Other robustness checks

In Table 4 we report a set of additional robustness checks. For ease of comparison, the table shows the estimated coefficients on MDD^+ and MDD^- from the main specification and from six alternative models. All regressions keep the same fixed effect and controls structure as the main model; the number of observations varies only because in each check we may have to apply some exclusion rules. In the last column we report, in percentage terms, the share of total revenue included in the subset.

We begin by replacing the baseline outcome, log revenue, with the log of the *landed weight*. This check removes the role of prices. The baseline dependent variable is the product of quantities and prices, and temperature shocks could in principle affect prices through changes in aggregate supply, quality, or market composition. If fixed effects adequately controlled for prices, the estimated temperature response should be similar when using quantities instead of revenue. Consistent with this prediction, the coefficients remain very stable.

We then assess whether the results depend on particularly vulnerable stocks, for which non-temperature pressures (such as overfishing or habitat degradation) could dominate and adjustment may be slow. In the specification labeled *Not endangered*, we exclude all species that the IUCN Red List classifies as *Critically Endangered*, *Endangered* or *Vulnerable* www.iucnredlist.org. In the specification labeled *Only resilient*, we exclude species with low or very low resilience, i.e., species with limited recovery potential based on biological traits such as growth, age of reproductive maturity, and average reproductive output (e.g. average number of eggs) (Froese et al., 2017). In both cases, coefficient estimates are very similar to those estimated in the main model.

Next, we test sensitivity to the exclusion of highly migratory species. If temperature shocks affect revenue through large-scale redistribution, especially for species that move across ocean basins or between distant regions, then excluding highly migratory species should alter the estimates. The *Not migratory* specification removes species classified as highly migratory in FishBase (e.g., tuna and swordfish). The results remain essentially unchanged.

In the *Only EEZ* specification we restrict the sample to catches taken within the Exclusive Economic Zones (EEZ) of EU member states. Arguably, both the enforcement and monitoring of the Common Fisheries Policy are less strict in distant regions than within the EU EEZs. This could affect reporting, targeting decisions, or compliance. Reassuringly, focusing only on areas within the EU EEZ does not significantly affect our estimates.

Finally, we test sensitivity to a highly flexible set of controls for species-specific spatial suitability by including in the model a thin-plate spline in latitude and longitude with 500 bases for each species. The estimates remain very close to those of our preferred model.

Supplemental Appendix D.4 reports an additional robustness check estimating the model across alternative time periods. This is important as the Mediterranean spatial reporting became fully enforced only in 2017, while UK vessels are observed only between 2014 and 2019 because of Brexit occurring in 2020. The estimates remain stable across all these subsamples.

Table 4: Coefficient estimation results for different robustness checks

Model	MDD^{+} ($\times$ 100)	MDD^{-} ($\times$ 100)	Obs (million)	revenue share (%)
Main	-0.132*** (0.013)	-0.044*** (0.012)	2.542	100
landed weight	-0.135*** (0.013)	-0.041*** (0.012)	2.542	100
Not endangered	-0.113*** (0.012)	-0.030** (0.012)	2.267	89
Only resilient	-0.138*** (0.013)	-0.035*** (0.014)	2.156	91
Not migratory	-0.134*** (0.013)	-0.049*** (0.014)	2.324	94
Only EEZ	-0.135*** (0.013)	-0.024* (0.014)	2.229	82
Flexible spatial spline	-0.152*** (0.013)	-0.054*** (0.010)	2.542	100

Clustered (cell) standard-errors in parentheses
*Signif. Codes: ***: 0.01, **: 0.05, *: 0.10*

7 Non linearities and heterogeneous effects

7.1 Non-linear effects

Equation (15) assumes a linear effect of MDD^{-}_{its} and MDD^{+}_{its} on (log) revenue. However, deviations from species' preferred temperatures could be increasingly harmful if, for instance, marine heatwaves generate proportionally larger biological impacts relative to moderate warming (K. E. Smith et al., 2023). To allow for a more flexible functional form, we also estimate a binned version of the temperature response function.

We partition daily temperatures into intervals defined relative to each species-specific thermal thresholds. Let $[TP_s^{\min}; TP_s^{\max}]$ denote the preferred temperature range for species s, and let TP_s^{*} denote the midpoint of this range, which we assume to be its *optimal temperature*. We define 1) a narrow *comfort zone* around TP_s^{*} as the temperature values within one quarter of the preferred-range width and 2) a broader *tolerance zone* as the remaining part of the preferred range. We also split the temperatures below $TP_s^{\min}$ and above $TP_s^{\max}$ into *moderate* and *extreme* exposure. Specifically, temperatures within $5°C$ of these thresholds are classified as moderate, while those more than $5°C$ beyond them are classified as extreme.

We then calculate the MDDs that belong within each one of these intervals. Using as reference the thermal range in the comfort zone, we indicate the exposure within the tolerance zone as MDD^{tol}_{its}, and the moderate and extreme exposure above and below the preferred thermal range as $MDD^{+,<5}_{its}$, $MDD^{+,>5}_{its}$, $MDD^{-,<5}_{its}$ and $MDD^{-,>5}_{its}$.

The resulting binned specification is:

$$f^{*}(\tau_{it}) \;=\; \beta^{tol}\, MDD^{tol}_{its} + \beta^{+,<5}\, MDD^{+,<5}_{its} + \beta^{+,>5}\, MDD^{+,>5}_{its} + \beta^{-,<5}\, MDD^{-,<5}_{its} + \beta^{-,>5}\, MDD^{-,>5}_{its}. \quad (18)$$

Table 5 reports the results of such specification while Figure 5 provides a graphical representation of the same estimates.

The estimated response function is strongly nonlinear on the heat exposure side. Moderate heat exposure, $MDD^{+,0-5}$, is negative and statistically significant, but the coefficient on extreme heat exposure, $MDD^{+,>5}$, is

much larger in absolute value. In particular, a one-hundred-unit increase in moderate heat exposure is associated with an approximately 4% decline in revenue, whereas the same increase in extreme heat exposure is associated with a revenue loss of about 30%. On the other hand, the cold-exposure response displays no significant evidence of non-linearity. Both cold-exposure bins are negative and statistically different from zero, and their magnitudes are very similar. Interestingly, revenue also responds to temperature realizations that remain within the species' preferred thermal range. The coefficient on MDD^{tol}, which captures exposure inside the preferred range but outside the narrow comfort zone around the optimum, is negative and statistically significant. Its magnitude, about -0.04, is slightly smaller than the cold-exposure coefficients and far below the extreme-heat coefficient, but still indicates that temperature realizations can have an impact even before they cross the biological tolerance bounds. This pattern is plausible because the preferred ranges reported in the biological literature are typically quite wide and, therefore, temperatures within the preferred range can also be meaningfully distant from the physiological optimum.[8]

Table 5: Binned specification

Dependent variable:	log(Revenue)				
Thermal exposure:	$MDD^{-,>5}$	$MDD^{-,<5}$	MDD^{tol}	$MDD^{+,<5}$	$MDD^{+,>5}$
Coefficient	-0.064^{***}	-0.055^{***}	-0.039^{***}	-0.037^{**}	-0.303^{***}
	(0.014)	(0.013)	(0.01)	(0.016)	(0.031)
Fit statistics					
Observations (millions)			2.542		
R^2			0.85		

Notes: Standard errors clustered at the cell level are reported in parentheses. All coefficients and standard errors are multiplied by 100. The regression includes the full set of fixed effects and controls used in the preferred specification, including trophic-interaction controls, species-specific habitat characteristics, and smooth spatial gradients. Exposure within the comfort zone is the omitted category. Significance levels: $^{***}p < 0.01$, $^{**}p < 0.05$, $^{*}p < 0.1$

[8]See Supplemental Appendix A.5 for details on the thermal ranges.

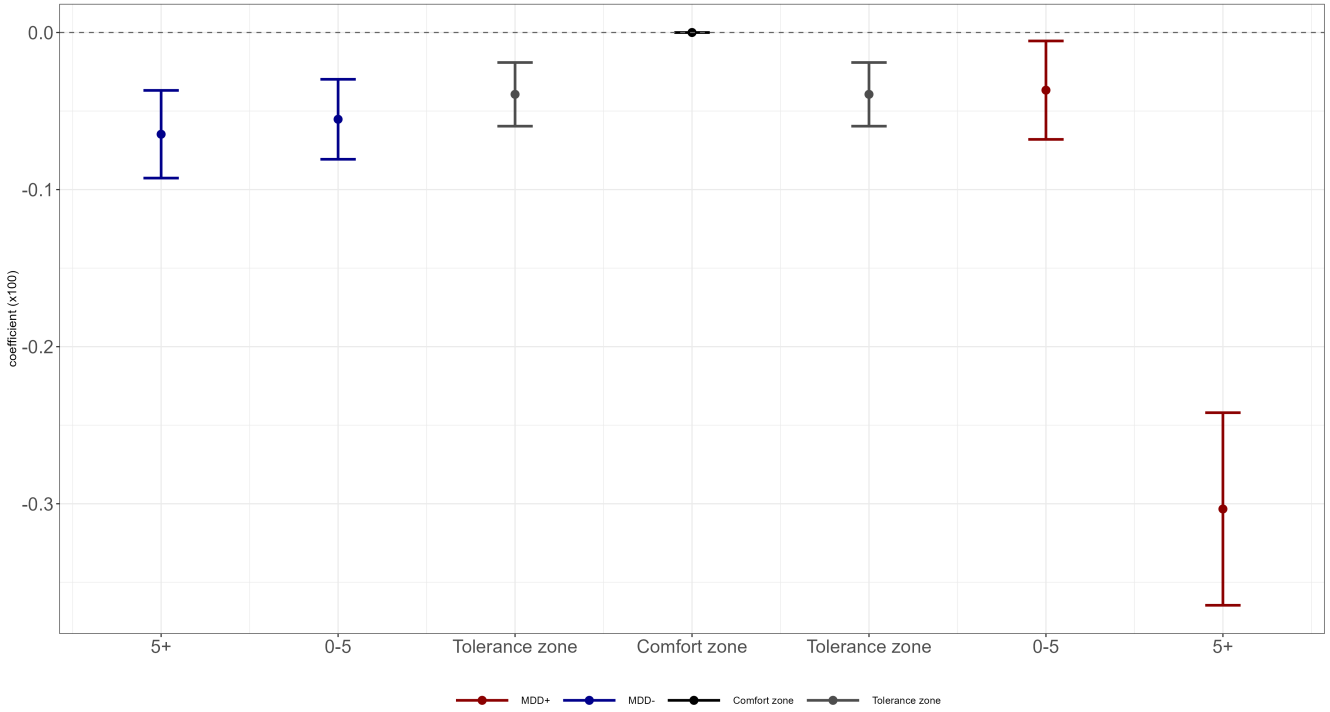


Figure 5: Non-linear effects of thermal exposure on fishing revenue. Error bars indicate 95% confidence intervals.

7.2 Ecological categories

We now investigate if impacts are heterogeneous across three broad ecological categories: pelagic fishes, demersal fishes, and invertebrates. Pelagic species inhabit the open water column and include species such as sardines and tuna. Demersal species live close to the seabed, often moving actively near the bottom, and include cod and hake. Invertebrates are mostly benthic organisms, such as scallops and clams. In terms of economic relevance in our data, invertebrates account for about 27% of revenue, pelagic species for approximately 40%, and demersal species for the remaining 33%.

Table 6 reports the results from interacting both MDD^+ and MDD^- with species' ecological category. Pelagic species experience sizable negative effects, equal to -0.093 for heat exposure and -0.042 for cold exposure. Demersal species exhibit the strongest response to thermal exposure. An additional 100 MDD^+ is associated with approximately a 14% decline in revenue, while the corresponding effect of MDD^- is -0.064. The stronger response of demersal species may reflect their more limited ability to avoid unfavorable local conditions, while pelagic species may have greater scope for horizontal and vertical movement within the water column. For invertebrates, the effect of heat exposure is also negative and statistically significant, indicating that this ecological group experiences revenue losses under warmer-than-preferred conditions. By contrast, the coefficient for cold exposure is smaller and not statistically different from zero, suggesting a weaker response to cold exposure relative to the other ecological groups.

Table 6: Heterogeneity by ecological category

Dependent variable:	log(Revenue)			
Ecological category:	Full sample	Pelagic	Demersal	Invertebrates
Thermal exposure				
MDD^{+} ($\times 100$)	-0.132^{***}	-0.093^{***}	-0.148^{***}	-0.064^{**}
	(0.013)	(0.015)	(0.015)	(0.027)
MDD^{-} ($\times 100$)	-0.044^{***}	-0.042^{***}	-0.064^{***}	-0.014
	(0.012)	(0.015)	(0.016)	(0.018)
Fit statistics				
Observations (millions)	2.542			
R^2	0.85			

Notes: Standard errors clustered at the cell level are reported in parentheses. All the specifications include the full set of fixed effects and controls used in the full model, including trophic-interaction controls, species-specific habitat characteristics, and smooth spatial gradients. Significance levels: $^{***}p < 0.01$, $^{**}p < 0.05$, $^{*}p < 0.1$.

7.3 Vertical mobility potential

Can species mitigate thermal exposure by moving vertically within the water column? The extent to which a species can use this margin depends on two factors: 1) its biological depth range and 2) the depth of the location where it is situated. Let $d_s^{\max}$ and $d_s^{\min}$ denote the maximum and minimum depths of the biological range reported for species s. We define *vertical mobility potential* (VMP) as the length of the species' depth range that is feasible in a given cell, capped by local bathymetry D_i.

$$VMP_{is} = \max\{0,\ \min\left(d_s^{\max},\ D_i\right) - d_s^{\min}\},$$

VMP is large when a species has a broad depth range and the local bathymetry allows that range to be realized.

Table 7 reports the estimates of an extension of the full model where the temperature exposure is interacted with three categories of VMP. Figure 6 reports the corresponding effects of heat and cold exposure for each category. The results provide evidence that vertical mobility moderates the effect of heat exposure. Relative to species with less than 100 meters of feasible vertical range, the heat exposure effect is less negative for both higher VMP categories. Most of this attenuation happens once species have access to at least 100 meters of feasible vertical range, with little additional difference offered by the deepest ranges. For cold exposure, we find no meaningful difference between the first two VMP bins, indicating that the marginal effect on revenue remains essentially unchanged up to 500 meters. However, where VMP is above 500 meters, the effect of cold exposure becomes less negative.

Table 7: Heterogeneity by vertical mobility potential

Dependent variable:	log(Revenue)		
Vertical mobility potential:	VMP_{0-100}	$VMP_{100-500}$	VMP_{500+}
Thermal exposure			
MDD^{+} ($\times 100$)	-0.144^{***}	-0.109^{***}	-0.112^{***}
	(0.013)	(0.013)	(0.014)
MDD^{-} ($\times 100$)	-0.048^{***}	-0.048^{***}	-0.026^{**}
	(0.012)	(0.012)	(0.012)
Fit statistics			
Observations (millions)		2.542	
R^2		0.85	

Notes: Each column reports the estimated effect of thermal exposure for the corresponding vertical mobility potential category. Standard errors clustered at the cell level are reported in parentheses. Each specification includes the full set of fixed effects and controls used in the full model, including trophic-interaction controls, species-specific habitat characteristics, and smooth spatial gradients. Significance levels: $^{***}p < 0.01$, $^{**}p < 0.05$, $^{*}p < 0.1$.

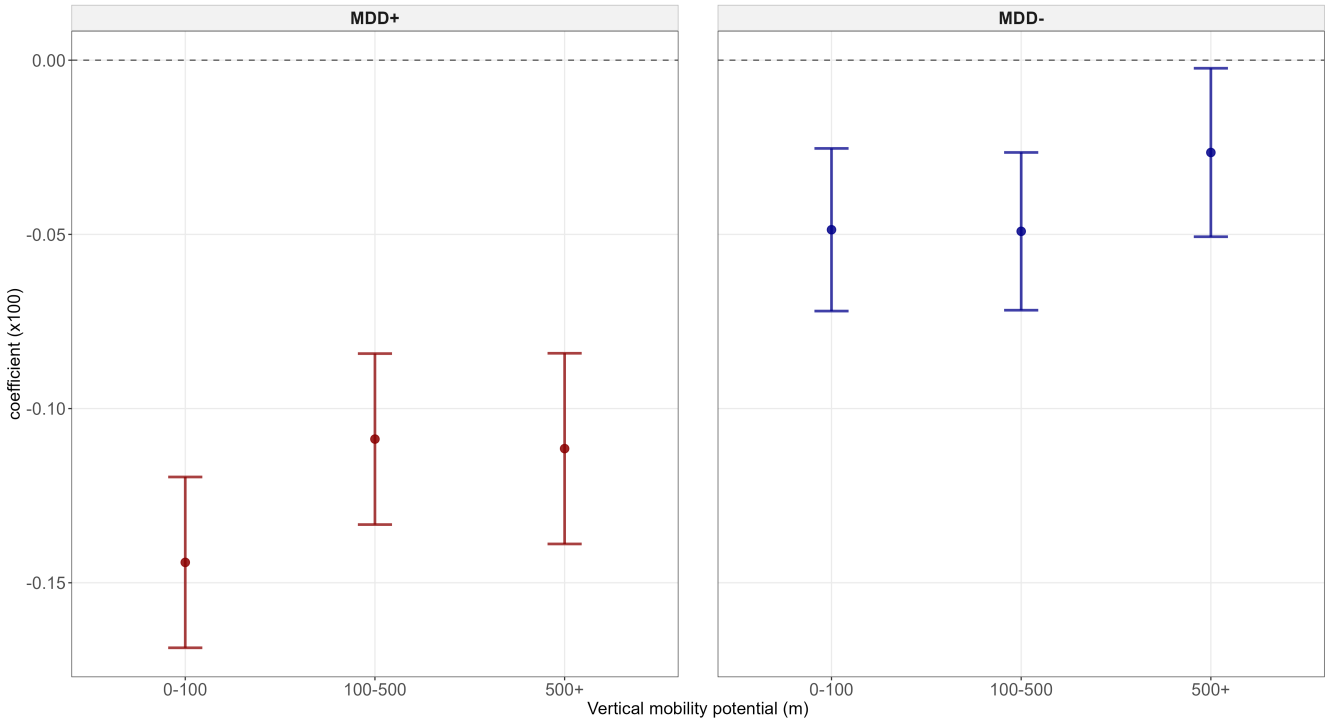


Figure 6: Mediating effect of vertical mobility potential on thermal exposure. The figure reports the implied marginal effects of hot and cold exposure across VMP bins, with 95% confidence intervals.

8 Climate change projections

8.1 Methods

Here we investigate the impact of future climate change on fisheries revenue by combining our full model (Table 1, column 3) with daily SST projections under two alternative emissions pathways: SSP-2.45 and SSP-3.70. For each grid cell and year in each climate scenario, we compute species-specific thermal exposure measures (MDD^+ and MDD^-). We then express projected exposure as deviations from the 2013-2022 baseline and translate these deviations into percentage revenue changes using the estimated coefficients. We obtain projected damages for each species by multiplying the predicted proportional change by the average cell-specific revenue observed during the baseline period. Finally, we aggregate the projected damages at the cell level by summing over all the species. Projecting differences from the 2013-2022 baseline holds fixed all the non-temperature determinants of revenue absorbed by our fixed effects (e.g., price conditions, fuel costs, regulations and enforcement, fleet composition, and other common shocks), so that our scenarios should be interpreted ceteris paribus and not as predictions of the future. To avoid extrapolating the estimated temperature-response function beyond the support of the data, we constrain projected thermal exposure to the range observed in the estimation sample, replacing values outside this range with the nearest observed boundary (Auffhammer et al., 2013; Fezzi & Bateman, 2015). This adjustment affects less than 0.1% of projected observations.

Considering the potential channels of fishers' adaptation, a key feature of our setting is that fishing activity conducted within the spatial boundaries of our analysis is regulated under the Common Fisheries Policy (and related bilateral agreements), whose operational objective is to keep exploitation rates consistent with MSY (EU, 2013). For our projections, this implies that adaptation operates within an institutional constraint. For each species, the management adjusts the aggregate harvest quota in response to stock conditions and scientific advice, while fishers can adapt only within the constraint implied by that quota. When quotas are fully utilized, additional fishing effort cannot offset temperature-induced reductions in the total allowable catch, as aggregate harvest is constrained by regulation. However, when quotas are not fully utilized, fishers may have greater scope to compensate for declining productivity by increasing effort or adjusting their fishing strategies. Unused quotas do not necessarily imply effective adaptation opportunities, as catches may remain constrained by stock availability, fishing costs, or other operational limitations. Nevertheless, where feasible, adjustments in fishing effort could provide a margin of adaptation, potentially mitigating some of the projected revenue losses associated with climate change.

Another potential margin of adaptation involves gradual shifts, such as expansion into new fishing grounds. In our projections, we exclude such spatial shifts and maintain the geographic boundaries defined by our data. This approach is akin to the assumption implemented in the agricultural economics literature, which holds total land area constant when calculating climate change projections (Burke & Emerick, 2016). Furthermore, a large-scale reallocation of effort across fishing grounds is unlikely since policy trends point toward greater spatial restrictions rather than expansion. Proposals to restrict fishing in the high seas are gaining traction (Roberts et al., 2025), and

marine protected areas are expanding globally (McDonald et al., 2024). Taken together, these forces suggest that wild fisheries are more likely to be compressed than to find substantial new space.

A final concern is that climate change may induce long-run shifts in species distributions. Our cell-level projections hold the species present in a cell fixed to those observed during the baseline years. In other words, in each given cell, species already present can decline significantly, potentially approaching zero, but species that are currently absent cannot enter the cell. The projections may therefore understate local species replacement as suitable habitats shift. Available evidence suggests such species displacements to be limited, with changes in species-distribution centroids or boundaries averaging approximately 5–7 km per year (García Molinos et al., 2016), making this feature unlikely to affect our results. However, we explore its relevance by recalculating our climate change projection at the management-area level, using the estimates in Table 3. Management areas combine, on average, more than 50 individual $0.5° \times 0.5°$ cells and have a median area of approximately 160,000 km^2. This aggregation allows projections to draw on a much broader set of species historically observed within each area and, therefore, allows much more significant species redistribution. The results, which are reported in Supplemental Appendix E, leave the main conclusions unchanged.

8.2 Projected impacts

Figure 7 presents predicted percentage changes for each of the two scenarios, grouped into three time windows (2026-2050, 2051-2075, and 2076-2100). Each boxplot represents the distribution of 25 values of yearly aggregated revenue changes and, therefore, illustrates year-to-year variability within each scenario and time frame and not model uncertainty. Median effects are negative in both scenarios and become more severe over time. In the first time period (2026-2050), median losses are modest, around 2% in both scenarios. By mid-century (2051-2075), damages increase to roughly 5% under SSP-2.45 and 6% under SSP-3.70. By the last quarter of the century (2076-2100), the divergence between the two scenarios becomes clearer: median losses are around 8% under SSP-2.45 and about 12% under SSP-3.70.

Figure 8 reports the same results as a continuous time series, expressed in billions of euros relative to the 2013-2022 baseline (baseline aggregate revenue in our study area is approximately 4.5 billion euros per year). Our projections show that the two scenarios remain relatively close in the first half of the century and diverge after mid-century. In the near term, ocean warming is limited and the reduction in cold exposure can partially offset the increase in heat exposure, yielding relatively small aggregate changes. As warming strengthens, heat exposure grows rapidly and dominates our impacts, since our estimated effects are markedly asymmetric. By the end of the century, losses reach around 430 million euros per year under SSP-2.45 and around 560 million euros per year under SSP-3.70. The shaded confidence intervals are obtained from 1,000 Monte Carlo simulations drawing the model coefficients from their estimated joint distribution. These intervals widen toward the end of the century as projected temperatures diverge from the current ones.

Figure 9 maps projected impacts at the cell level, highlighting the strong spatial heterogeneity across scenarios

and horizons (2051-2075 in the top panel; 2076-2100 in the bottom panel). In the open Atlantic, impacts display a clear north-south gradient. By mid-century (2051-2075), tropical and subtropical waters exhibit large projected losses under both SSP-2.45 and SSP-3.70, often exceeding 30% relative to the baseline. At higher latitudes, damages become milder and, in some locations, the impact of climate change is even positive. These gains are most visible under SSP-3.70, especially in the late-century period (2076-2100), where parts of the Arctic, sub-Arctic and mid-Atlantic experience increases on the order of 10% to 20%, consistent with reductions in cold exposure more than offsetting the increase in heat exposure. In contrast, coastal and semi-enclosed seas near Europe experience predominantly reductions in revenue across both scenarios, with damages intensifying in later decades. An important implication of this spatial pattern is distributional: the largest losses are concentrated in lower-latitude regions, especially along the West African Atlantic, where projected damages are particularly severe under SSP-3.70. Since these ocean regions tend to be the most accessible to developing countries along the West African coast, our results highlight the unequal burden of climate-change impacts. The figure reports cell-level point estimates, while in Table E.1 of Supplemental Appendix E we report the 95% confidence intervals for spatially aggregated impacts at the FAO-area level.

Finally, Figure 10 reports late-century (2076-2100) projections for the 15 species generating the highest baseline revenue. Most species experience substantial declines, but there is meaningful heterogeneity. For example, Norway lobster is projected to benefit slightly under SSP-3.70, reflecting the fact that its catches are concentrated in colder waters where reduced cold exposure can generate a positive impact. At the other extreme, blue and red shrimp and European pilchard are among the most heavily affected species, with median losses exceeding 25% under SSP-3.70. Other sizable late-century losses include Atlantic herring, European plaice, European sprat, Atlantic cod, common shrimp, and Atlantic horse mackerel. Under SSP-2.45, the ranking of affected species is broadly similar, although losses are less severe. Importantly, even relatively small percentage declines can translate into substantial absolute losses for high-value species such as Atlantic mackerel, which accounts for the largest share of baseline revenue.



Figure 7: Projected percentage change in revenue relative to the 2013-2022 baseline, aggregated over three 25-year periods (2026-2050, 2051-2075, 2076-2100) for each emissions pathway. Each boxplot summarizes 25 annual projections. Boxes indicate the interquartile range (25th–75th percentiles), the central line denotes the median, and whiskers extend to the full range of the observed values.

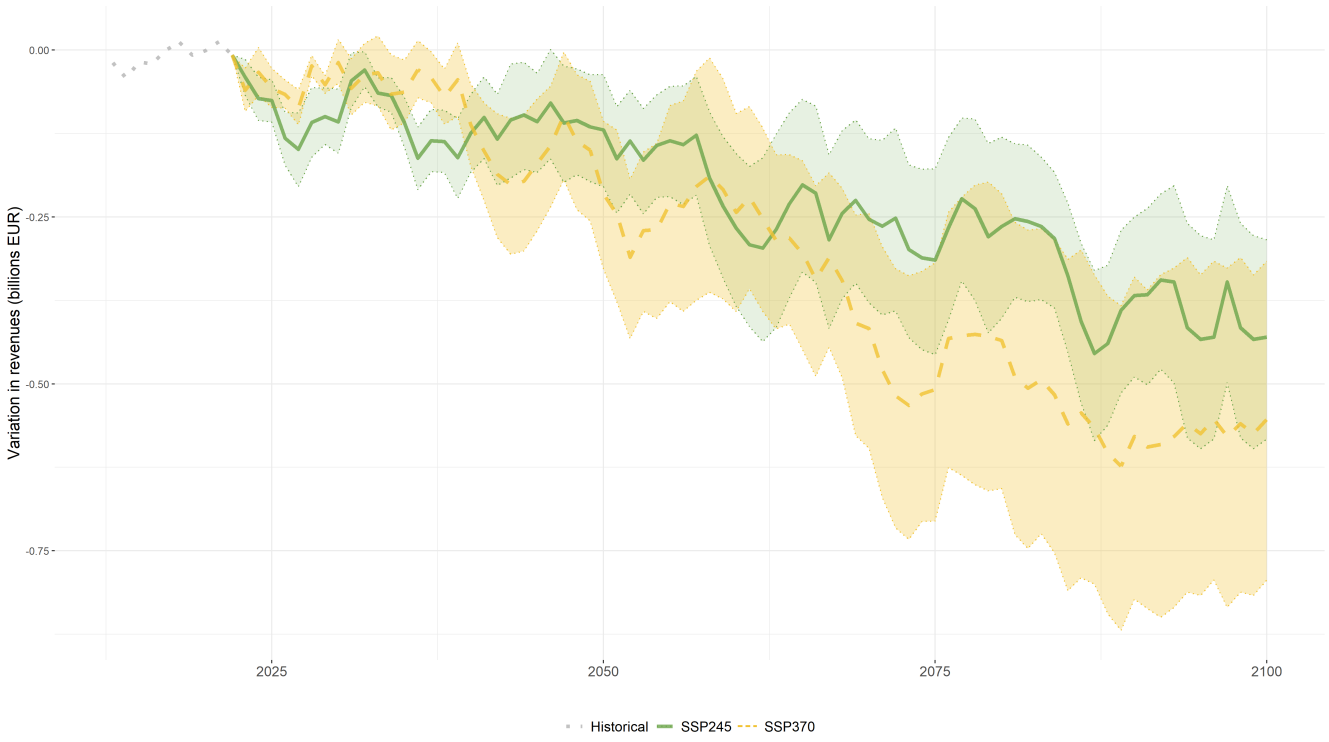


Figure 8: Aggregate projected change in annual revenue (billions of euros) relative to the 2013-2022 baseline, shown as a right-aligned 5-year moving average. Shaded bands indicate 95% confidence intervals computed through 1000 Monte Carlo simulations from the model's parameters. The gray-dotted line at the beginning of the time-series reports the same moving average from the climate model historical projections (2013-2022).

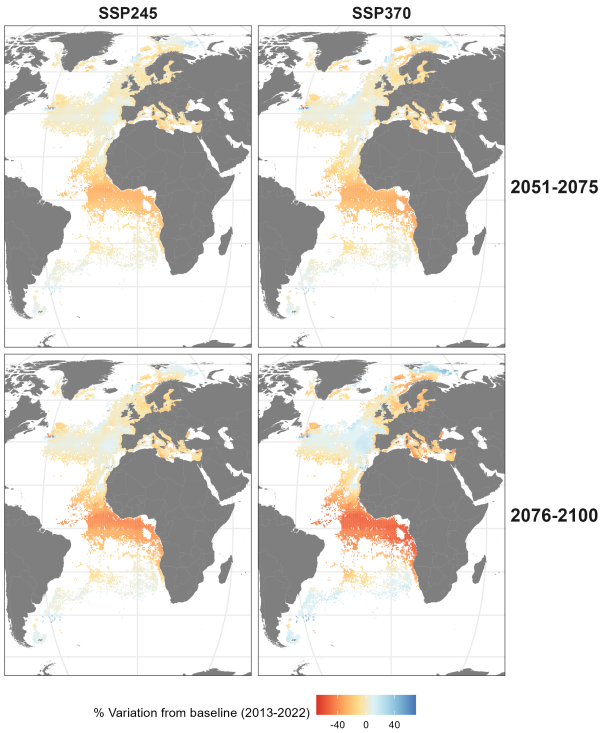


Figure 9: Spatial heterogeneity in projected revenue impacts at the cell level. Each panel maps the projected percentage change relative to the 2013-2022 baseline for a given emissions pathway and period (2051-2075 in the top row; 2076-2100 in the bottom row).

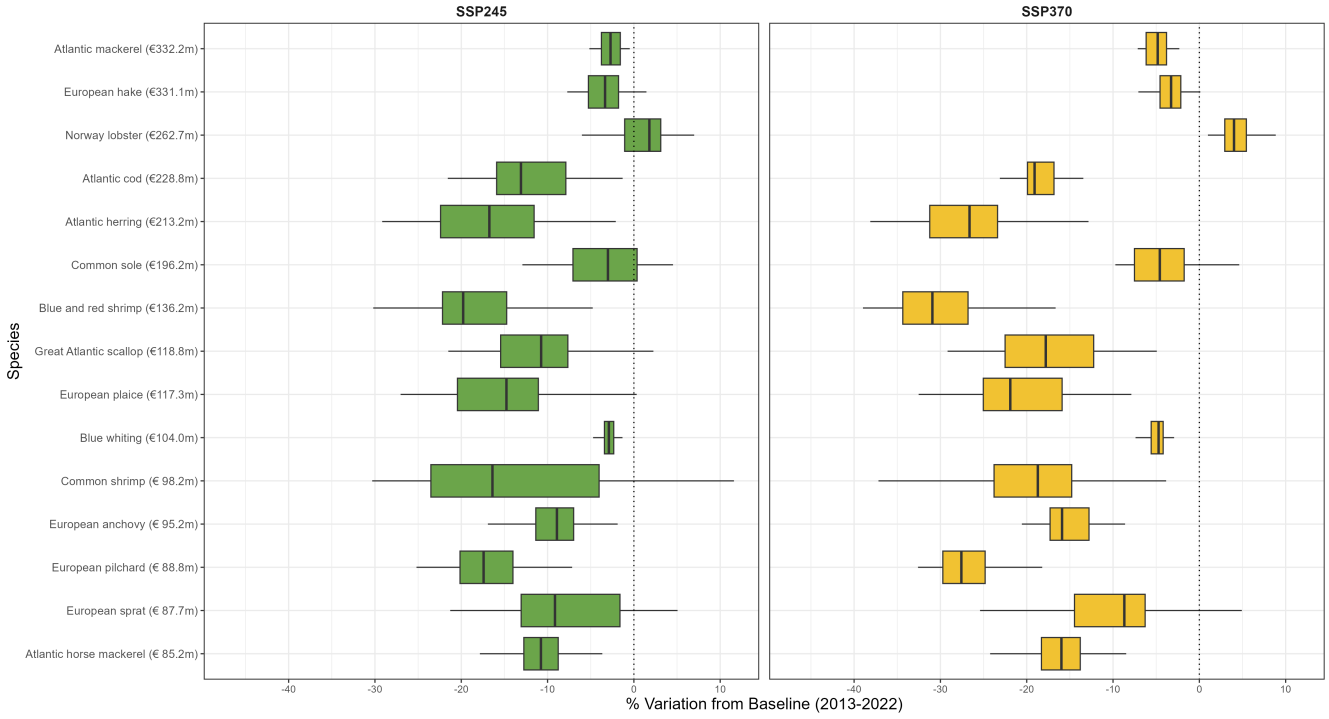


Figure 10: Late-century species-level projections (2076–2100) for the 15 species with the highest baseline revenue (baseline annual revenue reported in parentheses). For each emissions pathway, each boxplot summarizes 25 annual projections of the percentage change in revenue relative to the 2013–2022 baseline. Boxes indicate the interquartile range (25th–75th percentiles), the central line denotes the median, and whiskers extend to the full range of observed values.

9 Discussion and conclusion

This paper estimates the causal impact of ocean temperature on fisheries revenue. Exposure to temperatures outside a species' preferred thermal range affects its carrying capacity, ultimately reducing its stock biomass. Therefore, deviations from species' preferred temperature ranges, both colder and warmer, reduce revenue, but the impact of heat exposure is almost three times stronger than the impact of cold exposure. Prior evidence shows that low temperatures can slow feeding and growth, especially for warm-adapted species (Reid et al., 2022). On the other hand, heat exposure creates a broader set of risks including habitat disruption (for example through coral bleaching) and lower oxygen availability in the water column (Alfonso et al., 2021).

Our results show that heat exposure becomes especially damaging when temperatures exceed the upper bound of the thermal range by a large margin (i.e. more than 5°C). This pattern is consistent with evidence that extreme warming events, e.g. marine heatwaves, can trigger large and persistent disruptions in marine ecosystems (K. E. Smith et al., 2023). This is particularly relevant given that marine heatwaves are projected to become more frequent and intense under climate change (Frölicher et al., 2018).

We also show that a species' ability to move vertically within the water column mitigates the impact of thermal exposure, especially for heat anomalies. This is consistent with the idea that species can exploit the vertical temperature gradients to buffer the thermal stress. For this reason, incorporating the vertical thermal gradient in the characterization of exposure and responses may become increasingly important as deoxygenation alters habitat quality at depth (Fredston et al., 2023).

We also estimate meaningful heterogeneity across ecological groups. Demersal species, which live near the seabed, appear particularly vulnerable to both warming and cooling. Pelagic species, which occupy the open water column, are more resilient, plausibly because they can adjust their distribution more easily in response to temperature shifts. Finally, invertebrates, such as clams, cuttlefish or squid, show the highest resilience of all ecological categories we examined.

Turning to climate change impact projections, our scenarios provide a clear picture of how, ceteris paribus, climate change will affect fisheries. While magnitudes vary across scenarios and regions, the overall pattern points to negative aggregate impacts. We estimate a strong geographic heterogeneity, implying that climate change will create both winners and losers, as in other sectors such as agriculture (Auffhammer, 2018; Fezzi & Bateman, 2015; Schlenker et al., 2006). High-latitude and cold Atlantic regions may experience revenue gains, raising the importance of international cooperation and governance to manage shifting and newly accessible resources. By contrast, warmer ocean regions and enclosed seas such as the Mediterranean and Baltic are projected to face large losses, calling for region-specific adaptation strategies and support for vulnerable fishing communities.

From a policy perspective, this heterogeneity may suggest prioritizing adaptive management where risks are the greatest. In settings where warming shifts productivity across space and species, policies that facilitate adjustment, such as flexible quota allocations and incentives to diversify target portfolios, may reduce costs, though our study was

unable to test these adjustments directly. The divergence in outcomes across scenarios after 2050 also underscores the value of mitigation.

Our projections can be compared to earlier *simulation-based* studies of climate impacts on global fisheries (Barange et al., 2014; Cheung et al., 2010, 2021; Lam et al., 2016). These studies confirm our conclusion that climate change will generate both winners and losers, but our quantitative projections differ in important ways. Relative to such studies, our projections are less severe by mid century. In particular, compared with Lam et al. (2016), we estimate modest aggregate losses by 2050, and compared with Cheung et al. (2010) and Barange et al. (2014) we find weaker spatial heterogeneity at mid century, even though the end of century spatial pattern is qualitatively similar (losses in enclosed and low latitude seas and gains at higher latitudes). Our interpretation is that *simulation-based* approaches may overstate both positive and negative changes relative to what is implied by realized economic outcomes. This is consistent with the fact that such approaches typically abstract from adaptation margins.

Finally, our approach comes with its own caveats. First, because we project differences from the 2013-2022 baseline, our results are conditional on institutional and market conditions, including prices and demand conditions, input costs, and fleet composition. In the long run, these are all possible margins of adaptation. Second, while realized outcomes embed the short-run behavioral and institutional adjustments observed in the data, they do not capture slower, structural adaptations that may matter over longer horizons, such as major technological change, durable shifts in targeting and spatial access, or reforms to the Common Fisheries Policy that alter harvest caps and allocation rules. A natural extension for future research would be to refine our projections by explicitly modeling how fishing effort and spatial quota allocation respond to temperature, also beyond the geographical extent of our dataset.

References

Acevedo, S., Mrkaic, M., Novta, N., Pugacheva, E., & Topalova, P. (2020). The Effects of Weather Shocks on Economic Activity: What are the Channels of Impact? *Journal of Macroeconomics*, *65*, 103207. https://doi.org/10.1016/j.jmacro.2020.103207

Alfonso, S., Gesto, M., & Sadoul, B. (2021). Temperature increase and its effects on fish stress physiology in the context of global warming. *Journal of Fish Biology*, *98*(6), 1496–1508. https://doi.org/10.1111/jfb.14599

Alsan, M. (2015). The effect of the tsetse fly on african development. *American Economic Review*, *105*(1), 382–410. https://doi.org/10.1257/aer.20130604

Amemiya, T. (1984). Tobit models: A survey. *Journal of Econometrics*, *24*(1), 3–61. https://doi.org/https://doi.org/10.1016/0304-4076(84)90074-5

Angrist, J. D., & Pischke, J.-S. (2008). *Mostly harmless econometrics: An empiricist's companion*. Princeton University Press.

Assis, J., Fernández Bejarano, S. J., Salazar, V. W., Schepers, L., Gouvêa, L., Fragkopoulou, E., Leclercq, F., Vanhoorne, B., Tyberghein, L., Serrão, E. A., Verbruggen, H., & De Clerck, O. (2024). Bio-oracle v3.0: Pushing marine data layers to the cmip6 earth system models of climate change research. *Global Ecology and Biogeography*, *33*(4), e13813. https://doi.org/10.1111/geb.13813

Auffhammer, M. (2018). Quantifying Economic Damages from Climate Change. *Journal of Economic Perspectives*, *32*(4), 33–52. https://doi.org/10.1257/jep.32.4.33

Auffhammer, M., Hsiang, S. M., Schlenker, W., & Sobel, A. (2013). Using weather data and climate model output in economic analyses of climate change. *Rev. Environ. Econ. Pol.*, *7*(2), 181–198.

Auth, T. D., Daly, E. A., Brodeur, R. D., & Fisher, J. L. (2018). Phenological and distributional shifts in ichthyoplankton associated with recent warming in the northeast Pacific Ocean. *Global Change Biology*, *24*(1), 259–272. https://doi.org/10.1111/gcb.13872

Barange, M., Merino, G., Blanchard, J. L., Scholtens, J., Harle, J., Allison, E. H., Allen, J. I., Holt, J., & Jennings, S. (2014). Impacts of climate change on marine ecosystem production in societies dependent on fisheries. *Nature Climate Change*, *4*(3), 211–216. https://doi.org/10.1038/nclimate2119

Barbier, E. B. (2000). Valuing the environment as input: Review of applications to mangrove-fishery linkages. *Ecological Economics*, *35*(1), 47–61. https://doi.org/10.1016/S0921-8009(00)00167-1

Bilal, A., & Känzig, D. R. (2026). The macroeconomic impact of climate change: Global versus local temperature. *The Quarterly Journal of Economics*, *141*(2), 889–944. https://doi.org/10.1093/qje/qjag011

Burke, M., & Emerick, K. (2016). Adaptation to Climate Change: Evidence from US Agriculture [Publisher: American Economic Association]. *American Economic Journal: Economic Policy*, *8*(3), 106–140. https://doi.org/10.1257/pol.20130025

Burke, M., González, F., Baylis, P., Heft-Neal, S., Baysan, C., Basu, S., & Hsiang, S. (2018). Higher temperatures increase suicide rates in the United States and Mexico. *Nature Climate Change*, *8*(8), 723–729. https://doi.org/10.1038/s41558-018-0222-x

Cain, L., Hernandez-Cortes, D., Timmins, C., & Weber, P. (2024). Recent Findings and Methodologies in Economics Research in Environmental Justice [Publisher: The University of Chicago Press]. *Review of Environmental Economics and Policy*, *18*(1), 116–142. https://doi.org/10.1086/728100
doi: 10.1086/728100.

Card, D., & Dahl, G. B. (2011). Family Violence and Football: The Effect of Unexpected Emotional Cues on Violent Behavior*. *The Quarterly Journal of Economics*, *126*(1), 103–143. https://doi.org/10.1093/qje/qjr001

Carleton, T., & Hsiang, S. M. (2016). Social and economic impacts of climate [Publisher: American Association for the Advancement of Science (AAAS)]. *Science*, *353*(6304). https://doi.org/10.1126/science.aad9837

Carleton, T., Jina, A., Delgado, M., Greenstone, M., Houser, T., Hsiang, S., Hultgren, A., Kopp, R. E., McCusker, K. E., Nath, I., Rising, J., Rode, A., Seo, H. K., Viaene, A., Yuan, J., & Zhang, A. T. (2022). Valuing the Global Mortality Consequences of Climate Change Accounting for Adaptation Costs and Benefits [Publisher: Oxford University Press (OUP)]. *The Quarterly Journal of Economics*, *137*(4), 2037–2105. https://doi.org/10.1093/qje/qjac020

Chen, J., & Roth, J. (2024). Logs with zeros? some problems and solutions. *The Quarterly Journal of Economics*, *139*(2), 891–936. https://doi.org/10.1093/qje/qjad054

Cheung, W. W. L., Lam, V. W. Y., Sarmiento, J. L., Kearney, K., Watson, R., Zeller, D., & Pauly, D. (2010). Large-scale redistribution of maximum fisheries catch potential in the global ocean under climate change. *Global Change Biology*, *16*(1), 24–35. https://doi.org/10.1111/j.1365-2486.2009.01995.x

Cheung, W. W. L., Watson, R., & Pauly, D. (2013). Signature of ocean warming in global fisheries catch. *Nature*, *497*(7449), 365–368. https://doi.org/10.1038/nature12156

Cheung, W. W. L., Frölicher, T. L., Lam, V. W. Y., Oyinlola, M. A., Reygondeau, G., Sumaila, U. R., Tai, T. C., Teh, L. C. L., & Wabnitz, C. C. C. (2021). Marine high temperature extremes amplify the impacts of climate change on fish and fisheries. *Science Advances*, *7*(40), eabh0895. https://doi.org/10.1126/sciadv.abh0895

Cheung, W. W. L., Frölicher, T. L., Morgante, I., & Palacios-Abrantes, J. (2026). Large fisheries declines linked to compound and extreme climate events. *Nature Communications*, *17*(1), 8897. https://doi.org/10.1038/s41467-026-77077-z

Christensen, V., & Walters, C. J. (2004). Ecopath with ecosim: Methods, capabilities and limitations [Placing Fisheries in their Ecosystem Context]. *Ecological Modelling*, *172*(2), 109–139. https://doi.org/https://doi.org/10.1016/j.ecolmodel.2003.09.003

Costello, C., Ovando, D., Hilborn, R., Gaines, S. D., Deschenes, O., & Lester, S. E. (2012). Status and Solutions for the World's Unassessed Fisheries. *Science*, *338*(6106), 517–520. https://doi.org/10.1126/science.1223389

Costello, C., Cao, L., Gelcich, S., Cisneros-Mata, M. Á., Free, C. M., Froehlich, H. E., Golden, C. D., Ishimura, G., Maier, J., Macadam-Somer, I., Mangin, T., Melnychuk, M. C., Miyahara, M., De Moor, C. L., Naylor, R., Nøstbakken, L., Ojea, E., O'Reilly, E., Parma, A. M., ... Lubchenco, J. (2020). The future of food from the sea. *Nature*, *588*(7836), 95–100. https://doi.org/10.1038/s41586-020-2616-y

Dell, M. (2010). The persistent effects of peru's mining mita. *Econometrica*, *78*(6), 1863–1903. https://doi.org/https://doi.org/10.3982/ECTA8121

Dell, M., Jones, B. F., & Olken, B. A. (2012). Temperature Shocks and Economic Growth: Evidence from the Last Half Century. *American Economic Journal: Macroeconomics*, *4*(3), 66–95. https://doi.org/10.1257/mac.4.3.66

Dell, M., Jones, B. F., & Olken, B. A. (2014). What Do We Learn from the Weather? The New Climate-Economy Literature [Publisher: American Economic Association]. *Journal of Economic Literature*, *52*(3), 740–798. https://doi.org/10.1257/jel.52.3.740

Deschênes, O., & Greenstone, M. (2011). Climate Change, Mortality, and Adaptation: Evidence from Annual Fluctuations in Weather in the US [Publisher: American Economic Association]. *American Economic Journal: Applied Economics*, *3*(4), 152–185. https://doi.org/10.1257/app.3.4.152

Dunne, J. P., Horowitz, L. W., Adcroft, A. J., Ginoux, P., Held, I. M., John, J. G., Krasting, J. P., Malyshev, S., Naik, V., Paulot, F., Shevliakova, E., Stock, C. A., Zadeh, N., Balaji, V., Blanton, C., Dunne, K. A., Dupuis, C., Durachta, J., Dussin, R., ... Zhao, M. (2020). The GFDL Earth System Model Version 4.1 (GFDL-ESM 4.1): Overall Coupled Model Description and Simulation Characteristics. *Journal of Advances in Modeling Earth Systems*, *12*(11), e2019MS002015. https://doi.org/10.1029/2019MS002015

Durant, J. M., Molinero, J.-C., Ottersen, G., Reygondeau, G., Stige, L. C., & Langangen, Ø. (2019). Contrasting effects of rising temperatures on trophic interactions in marine ecosystems. *Scientific Reports*, *9*(1), 15213. https://doi.org/10.1038/s41598-019-51607-w

FAO. (2024, June). *The State of World Fisheries and Aquaculture 2024*. https://doi.org/10.4060/cd0683en

FAO. (2025, June). *Review of the state of world marine fishery resources – 2025*. https://doi.org/10.4060/cd5538en

Feir, D. L., Gillezeau, R., & Jones, M. E. C. (2024). The slaughter of the bison and reversal of fortunes on the great plains. *The Review of Economic Studies*, *91*(3), 1634–1670. https://doi.org/10.1093/restud/rdad060

Fezzi, C., & Bateman, I. (2015). The Impact of Climate Change on Agriculture: Nonlinear Effects and Aggregation Bias in Ricardian Models of Farmland Values [Publisher: University of Chicago Press]. *Journal of the Association of Environmental and Resource Economists*, *2*(1), 57–92. https://doi.org/10.1086/680257

Fowlie, M., Greenstone, M., & Wolfram, C. (2018). Do energy efficiency investments deliver? evidence from the weatherization assistance program. *The Quarterly Journal of Economics*, *133*(3), 1597–1644. https://doi.org/10.1093/qje/qjy005

Frank, E., & Sudarshan, A. (2024). The social costs of keystone species collapse: Evidence from the decline of vultures in india. *American Economic Review*, *114*(10), 3007–40. https://doi.org/10.1257/aer.20230016

Fredston, A. L., Cheung, W. W. L., Frölicher, T. L., Kitchel, Z. J., Maureaud, A. A., Thorson, J. T., Auber, A., Mérigot, B., Palacios-Abrantes, J., Palomares, M. L. D., Pecuchet, L., Shackell, N. L., & Pinsky, M. L. (2023). Marine heatwaves are not a dominant driver of change in demersal fishes. *Nature*, *621*(7978), 324–329. https://doi.org/10.1038/s41586-023-06449-y

Froese, R., Demirel, N., Coro, G., Kleisner, K. M., & Winker, H. (2017). Estimating fisheries reference points from catch and resilience. *Fish and Fisheries*, *18*(3), 506–526. https://doi.org/10.1111/faf.12190

Frölicher, T. L., Fischer, E. M., & Gruber, N. (2018). Marine heatwaves under global warming. *Nature*, *560*(7718), 360–364. https://doi.org/10.1038/s41586-018-0383-9

Gaines, S. D., Costello, C., Owashi, B., Mangin, T., Bone, J., Molinos, J. G., Burden, M., Dennis, H., Halpern, B. S., Kappel, C. V., Kleisner, K. M., & Ovando, D. (2018). Improved fisheries management could offset many negative effects of climate change. *Science Advances*, *4*(8), eaao1378. https://doi.org/10.1126/sciadv.aao1378

García Molinos, J., Halpern, B. S., Schoeman, D. S., Brown, C. J., Kiessling, W., Moore, P. J., Pandolfi, J. M., Poloczanska, E. S., Richardson, A. J., & Burrows, M. T. (2016). Climate velocity and the future global redistribution of marine biodiversity. *Nature Climate Change*, *6*(1), 83–88. https://doi.org/10.1038/nclimate2769

Gordon, H. S. (1954). The economic theory of a common-property resource: The fishery. *Journal of Political Economy*, *62*(2), 124–142.

Graff Zivin, J., & Neidell, M. (2014). Temperature and the Allocation of Time: Implications for Climate Change. *Journal of Labor Economics*, *32*(1), 1–26. https://doi.org/10.1086/671766

Harari, M., & Ferrara, E. L. (2018). Conflict, Climate, and Cells: A Disaggregated Analysis [Publisher: MIT Press - Journals]. *The Review of Economics and Statistics*, *100*(4), 594–608. https://doi.org/10.1162/rest_a_00730

Hoegh-Guldberg, O., & Bruno, J. F. (2010). The Impact of Climate Change on the World's Marine Ecosystems. *Science*, *328*(5985), 1523–1528. https://doi.org/10.1126/science.1189930

Hogan, D., & Schlenker, W. (2024). Empirical approaches to climate change impact quantification [ISSN: 3050-7294]. In *Handbook of the Economics of Climate Change* (pp. 53–111). Elsevier. https://doi.org/10.1016/bs.hesecc.2024.10.006

Hsiang, S. (2016). Climate Econometrics. *Annual Review of Resource Economics*, *8*(1), 43–75. https://doi.org/10.1146/annurev-resource-100815-095343

Huang, B., Liu, C., Banzon, V., Freeman, E., Graham, G., Hankins, B., Smith, T., & Zhang, H.-M. (2021). Improvements of the Daily Optimum Interpolation Sea Surface Temperature (DOISST) Version 2.1. *Journal of Climate*, *34*(8), 2923–2939. https://doi.org/10.1175/JCLI-D-20-0166.1

Kaiser, Michel J., Attrill, Martin J., Jennings, Simon, Thomas, David N., & Barnes, David K. A. (2020). *Marine ecology: Processes, systems, and impacts* (3rd ed). Oxford university press.

Lam, V. W. Y., Cheung, W. W. L., Reygondeau, G., & Sumaila, U. R. (2016). Projected change in global fisheries revenues under climate change. *Scientific Reports*, *6*(1), 32607. https://doi.org/10.1038/srep32607

McDonald, G., Bone, J., Costello, C., Englander, G., & Raynor, J. (2024). Global expansion of marine protected areas and the redistribution of fishing effort. *Proceedings of the National Academy of Sciences*, *121*(29), e2400592121. https://doi.org/10.1073/pnas.2400592121

Moscona, J., & Sastry, K. A. (2023). Does directed innovation mitigate climate damage? evidence from u.s. agriculture. *The Quarterly Journal of Economics*, *138*(2), 637–701. https://doi.org/10.1093/qje/qjac039

Palomares, M. L. D., & Pauly, D. (2014). West African marine ecosystems: Models and fisheries impacts. [Publisher: Fisheries Centre. University of British Columbia Version Number: 1]. https://doi.org/10.14288/1.0074805

Piroddi, C., Coll, M., Steenbeek, J., Macias Moy, D., & Christensen, V. (2015). Modelling the Mediterranean marine ecosystem as a whole: Addressing the challenge of complexity. *Marine Ecology Progress Series*, *533*, 47–65. https://doi.org/10.3354/meps11387

Rees, T. (2003). "C-Squares," A New Spatial Indexing System and its Applicability to the Description of Oceanographic Datasets. *Oceanography*, *16*(1), 11–19. https://doi.org/10.5670/oceanog.2003.52

Reid, C. H., Patrick, P. H., Rytwinski, T., Taylor, J. J., Willmore, W. G., Reesor, B., & Cooke, S. J. (2022). An updated review of cold shock and cold stress in fish. *Journal of Fish Biology*, *100*(5), 1102–1137. https://doi.org/10.1111/jfb.15037

Riahi, K., Van Vuuren, D. P., Kriegler, E., Edmonds, J., O'Neill, B. C., Fujimori, S., Bauer, N., Calvin, K., Dellink, R., Fricko, O., Lutz, W., Popp, A., Cuaresma, J. C., Kc, S., Leimbach, M., Jiang, L., Kram, T., Rao, S., Emmerling, J., ... Tavoni, M. (2017). The Shared Socioeconomic Pathways and their energy, land use, and greenhouse gas emissions implications: An overview. *Global Environmental Change*, *42*, 153–168. https://doi.org/10.1016/j.gloenvcha.2016.05.009

Roberts, C. M., Dyer, E., Earle, S. A., Forrest, A., Hawkins, J. P., Hoegh-Guldberg, O., Meeuwig, J. J., Pauly, D., Pimm, S. L., Sumaila, U. R., Rockström, J., & Lynas, M. (2025). Why we should protect the high seas from all extraction, forever. *Nature*, *642*(8066), 34–37. https://doi.org/10.1038/d41586-025-01665-0

Schlenker, W., Hanemann, W. M., & Fisher, A. C. (2006). The Impact of Global Warming on U.S. Agriculture: An Econometric Analysis of Optimal Growing Conditions. *Review of Economics and Statistics*, *88*(1), 113–125. https://doi.org/10.1162/rest.2006.88.1.113

Shrader, J. G. (2023). Improving climate damage estimates by accounting for adaptation. *Working paper*.

Smith, K. E., Burrows, M. T., Hobday, A. J., King, N. G., Moore, P. J., Sen Gupta, A., Thomsen, M. S., Wernberg, T., & Smale, D. A. (2023). Biological Impacts of Marine Heatwaves. *Annual Review of Marine Science*, *15*(1), 119–145. https://doi.org/10.1146/annurev-marine-032122-121437

Smith, M. D. (2005). State dependence and heterogeneity in fishing location choice. *Journal of Environmental Economics and Management*, *50*(2), 319–340. https://doi.org/10.1016/j.jeem.2005.04.001

Somanathan, E., Somanathan, R., Sudarshan, A., & Tewari, M. (2021). The Impact of Temperature on Productivity and Labor Supply: Evidence from Indian Manufacturing. *Journal of Political Economy*, *129*(6), 1797–1827. https://doi.org/10.1086/713733

Sumaila, U. R., Cheung, W. W. L., Lam, V. W. Y., Pauly, D., & Herrick, S. (2011). Climate change impacts on the biophysics and economics of world fisheries. *Nature Climate Change*, *1*(9), 449–456. https://doi.org/10.1038/nclimate1301

Tebaldi, C., Debeire, K., Eyring, V., Fischer, E., Fyfe, J., Friedlingstein, P., Knutti, R., Lowe, J., O'Neill, B., Sanderson, B., Van Vuuren, D., Riahi, K., Meinshausen, M., Nicholls, Z., Tokarska, K. B., Hurtt, G., Kriegler, E., Lamarque, J.-F., Meehl, G., … Ziehn, T. (2021). Climate model projections from the Scenario Model Intercomparison Project (ScenarioMIP) of CMIP6. *Earth System Dynamics*, *12*(1), 253–293. https://doi.org/10.5194/esd-12-253-2021

Tobin, J. (1958). Estimation of relationships for limited dependent variables. *Econometrica*, *26*(1), 24–36. Retrieved July 22, 2026, from http://www.jstor.org/stable/1907382

Ulanowicz, R., & Puccia, C. (1990). Mixed trophic impacts in ecosystems. *Coenoses*, *5*(1), 7–16. Retrieved July 21, 2026, from http://www.jstor.org/stable/43461017

Van Vuuren, D. P., O'Neill, B. C., Tebaldi, C., Sanderson, B. M., Chini, L. P., Friedlingstein, P., Hasegawa, T., Riahi, K., Govindasamy, B., Bauer, N., Eyring, V., Fall, C. M. N., Frieler, K., Gidden, M. J., Gohar, L. K., Högner, A., Jones, A. D., Kikstra, J., King, A., … Ziehn, T. (2026). The scenario model intercomparison project for CMIP7 (ScenarioMIP-CMIP7). *Geosci. Model Dev.*, *19*(7), 2627–2656.

Waldinger, M. (2022). The economic effects of long-term climate change: Evidence from the little ice age. *Journal of Political Economy*, *130*(9), 2275–2314. https://doi.org/10.1086/720393

Wooldridge, J. M. (2002). *Econometric analysis of cross section and panel data*. MIT Press.